Evaluation of Storminess by Early 20th Century Atmospheric Data from Signal Stations along the German Coastline

Dissertation
zur Erlangung des Doktorgrades
der Naturwissenschaften im Fachbereich
Erdsystemwissenschaften
der Universität Hamburg

vorgelegt von
Dörte Wagner

aus
Hannover

Hamburg, 2016

Gutachter: Prof. Dr. Hans von Storch
Dr. Birger Tinz
Disputation: 20.01.2017

Abstract

This work presents, for the first time, an analysis of signal station atmospheric observation data and their first evaluations. It shows that the signal station data has a benefit for scientific research in regard to the evaluation of storminess especially in the early 20th century along the German coastline. The Deutscher Wetterdienst (DWD) in Hamburg had archived handwritten annual journals of meteorological observational data from 164 signal stations. These data contain long-term time series of wind observations from the coast of the German Bight and the southern Baltic Sea covering a period of up to 120 years in the period from 1877 to 1999. The data allows studies of regional meteorological conditions to be made with greatly improved spatial resolution. The wind and Sea Level Pressure (SLP) data of selected signal stations along the German Bight and the southern Baltic Sea coast extend the monitoring network in maritime regions in time and space and show a spatial data homogeneity. After a homogenization in time, the data can also be used for long-term trend analysis, especially for storminess estimation in the German Bight and southern Baltic Sea region.

Long-term time series of wind data are often inhomogeneous. For an estimation of the change in storminess, in combination with storm surges along the German coastline, long-term time series of atmospheric observation data are necessary. Historical observation data could also improve the results of models and reanalyses.

The wind and SLP data of signal stations are spatially homogeneous, which is shown by an analysis of two historical storm surges at the German Bight and the southern Baltic Sea coast. The detection of inhomogeneties and the homogenization of SLP observation data from the signal stations is done from 15 selected stations by the Standard Normal Homogeneity Test (SNHT). The analysis of high percentile time series of the geostrophic wind for three triangles in the German Bight and the western Baltic Sea is done with observation and reanalysis data. The following data are used: SYNOP-data, as well as different observation data and the data of the regional reanalysis coastDat, and the global reanalysis National Center for Environmental Prediction (NCEP)/National Center for Atmospheric Research (NCAR). The analysis of the percentiles of the geostrophic wind show the potential for the use of signal station data for an extension of time series. The benefit of long-term wind observation is shown by an analysis of the time series of wind data over

120 years at Travemünde station.

Zusammenfassung

In dieser Arbeit werden die atmosphärischen Beobachtundsdaten von den Signalstationen erstmals vorgestellt und ihre erste Auswertung durchgeführt. Es wird gezeigt, dass die Signalstationsdaten einen Gewinn zur wissenschaftlichen Forschung im Zusammenhang mit der Einschätzung der Sturmhäufigkeit insbesondere im frühen 20. Jahrhundert an den Deutschen Küsten liefern. Der Deutsche Wetterdienst (DWD) in Hamburg archiviert handgeschriebene Jahrbücher meteorologicher Beobachtungsdaten von 164 Signalstationen. Diese Daten beinhalten Langzeit-Zeitreihen von Windbeobachtungen an den Küsten der Deutschen Bucht und der südlichen Ostsee von bis zu 120 Jahren im Zeitabschnitt von 1877 bis 1999. Die Daten erlauben Studien regionaler meteorologischer Bedingungen mit einer deutlich verbesserten räumlichen Auflösung. Wind und Luftdruckdaten ausgewählter Signalstationen entlang der Küste der Deutschen Bucht und der südlichen Ostsee erweitern das Beobachtungsnetzwerk in maritimen Regionen zeitlich und räumlich und zeigen eine zeitliche Homogenität der Daten. Nach der zeitlichen Homogenisierung können die Daten auch für Trend-Untersuchungen genutzt werden, besonders zur Abschätzung der Stürmigkeit in der Deutschen Bucht und der südlichen Ostsee.
Langzeit-Zeitreihen von Winddaten sind häufig inhomogen. Zur Abschätzung der Änderung der Stürmigkeit in Verbindung mit Sturmfluten entlang der deutschen Küstenlinie sind Langzeit-Zeitreihen meteorologischer Beobachtungsdaten notwendig. Historische Beobachtungsdaten können zudem Modell- und Reanalyseergebnisse verbessern.
Dass die Wind- und Luftdruckdaten der Signalstationen räumlich homogen sind, wird anhand der Analyse zweier historischer Sturmfluten an der Küste der Deutschen Bucht und der südlichen Ostsee gezeigt. Der Nachweis von Inhomogenitäten und die Homogenisierung der beobachteten Luftdruckdaten von Signalstationen wurde für 15 ausgewählte Stationen mit dem Standard Normal Homogeneity Test (SNHT) durchgeführt. Die Analyse von Zeitreihen hoher Perzentile des geostrophischen Windes wird für drei Dreiecke in der Deutschen Bucht und der westlichen Ostsee mit Beobachtungs- und Reanalysedaten durchgeführt. Als Beobachtungsdaten werden SYNOP-Daten und Daten der regionalen Reanalyse coastDat und der globalen Reanalyse NCEP/NCAR genutzt. Die Analyse der Perzentile des geostrophischen Windes zeigen das Potenzial von Signalstationsdaten für Langzeitreihen. Der

Gewinn von Langzeit-Beobachtungen des Windes wird anhand der Analyse von Zeitreihen über 120 Jahre von der Station Travemünde gezeigt.

Contents

1 Introduction

The current discussion on climate change and climate variability of extreme events in the atmosphere already includes air temperature rising in combination with green house gases, although the question on variability in storminess is a temporary discussion topic (Feser et al., 2015).
The risk of storm surges occuring as a consequence of strong winds is one of the most dangerous natural risks for the population at coastal areas with the risk of significant losses of life and property (Gönnert et al. (2001) and Petersen and Rohde (1977)). For the research area of the German Bight and the German coasts of the Baltic Sea, high wind speeds, in combination with a permanent wind direction from North-West for the German Bight and from North-East for the southern Baltic Sea, lead to a high risk of storm surges (von Storch and Worth, 2011). Historical storm surges at the German coasts are listed in Jensen and Müller-Navarra (2008). At the German North Sea coast, the first known storm surge can be dated back to 340 b.c., followed by 26 storm surges before 1900. In the 20th century at least 14 storm surges are known until 2007. The storm surge in 1906 at the German Bight is said to be the storm surge with the highest tidal high water until then. The catastrophical storm surge that occured in Hamburg in 1962 sacrificed hundreds of people's lives (von Storch and Worth, 2011). At the German Baltic Sea coast 22 storm surges occured from 1044 until 1900. After 1900, seven storm surges occured at the German Bight until 1995 with the strongest in 1976 (Jensen and Müller-Navarra, 2008).
Long-term trends of storminess can be derived by long-term time series. Historical long-term time series of wind speed are rarely homogeneous and consistent. The question about the change in storminess during the last century is linked with the change in storm surges. A high number of studies show inconsistent results for trend analysis for the North Atlantic and north-western Europe (Feser et al., 2015). The data used for this studies are observation data, reanalysis or model data (e.g. Bärring and Fortuniak (2009), Smits et al. (2005) and Beniston and Coauthors (2007)). Moreover, the use of proxy data is used for the calculation of long-term time series of geostrophic wind.
Historical observation data are valuable to improve the trend analysis of long-term time series of storminess and are also needed as an input for reanalysis.

An introduction to the coastal historical observation data, reanalysis and the geostrophic wind is given in the following sections. This chapter ends with the thesis objectives and a thesis outline.

1.1 Coastal Historical Observation Data

A set of different historical atmospheric observation data for coastal areas, especially for the German Bight and the southern Baltic Sea, is available. These are the dataset of SYNOP-data of the DWD data base, the newly digitized signal station data and the Marine Environmental Monitoring Network (MARNET) of the Bundesamt für Seeschifffahrt und Hydrografie (BSH), in combination with ship observations.

1.1.1 German Coastal Observation Data

SYNOP-Observation Data
The SYNOP-data are hourly observation data of meteorological parameters which enter the daily weather forecast. In Germany 211 stations belong to the network. 34 stations are owned by the Geoinformationsdienst der Bundeswehr (GeoInfoDBw) (DWD, 2016a). An overview of the network in North Germany is mapped in Fig. 1.1. Eight parameters are observed: SLP, air temperature, humidity, wind direction and speed, precipitation, snow depth and radiation budget. The data are encoded by the SYNOP-code. In recent years, the Binary Universal Form for the Representation of meteorological data (BUFR), created by the World Meteorological Organisation (WMO), replaces the SYNOP-code in consequence of a more simple handling of BUFR WMO (2016). The so-called SYNOP-data are available at the DWD-database for the the period from about 1960 to present.

MARNET and ship observations
The MARNET is a network of oceanographic and meteorological observation stations in the German Bight and the German part of the Baltic Sea. It is operated by the BSH. The atmospheric observation data are measured at 13 stations. These stations consist of light vessels, buoys and research platforms (called FINO). The disadvantages of the data of MARNET for long-term trend analysis are outages and too short series.

Figure 1.1.: Locations of SYNOP-Observation stations in North Germany. Stations signed with a red quadrate are climate reference stations, the red triangle stations with partly personal observation, the green quadrate indicate a GeoInfoDBw-Station with 24h personal observation and the green triangle a GeoInfoDBw-station with partly personal observation. The blue marks indicate stations of the DWD with an automatic observation.

Millions of data records from sailing ships, steamers and light vessels are archived at the DWD in Hamburg and were collected by the German Naval Observatory. In total, there are 37 000 logbooks with records dating back to the 18th century. Also, contemporary meteorological observations are done by ships to collect offshore weather information during their voyages (Kaspar et al., 2015). These data are stored in the DWD database. The disadvantage of these data is the inconsistance in time and space and therefore they are not valuable for long-term estimations.

1.1.2 Signal Station Data

The DWD houses a huge archive of historical meteorological observation data, measured by so-called signal stations along the German coastline. The signal stations were built along the German coastline for warning the population of upcoming storms by optical signals. The observation data started in 1887 and ended in 1999. In addition to wind observation data, SLP are

available from 1887 to 1939, which can be used for the calculation of the geostrophic wind as a proxy for the real wind. These data are presented and analyzed for the first time in this thesis. A detailed introduction of the signal station data is given in Section 2.

Global Signal Station

Signal stations exist or existed all over the world with different functions. In the 1880's the company Lloyd's formed a network of signal stations in the UK with 27 stations. The first station was built in the UK in Cornwall at the most southern point of England and is called the Lloyd's signal station. The station is described as a white washed two-story 9.1 m height building with a mast for flag signals at its top. The station was established in 1872 and closed in 1993. Weather messages were transmitted by using recognized flags. Also, lamps as night signals were used to communicate with vessels. The ships sent semaphore messages that could relay to their destination port by telecomunication (ET, 2016). In the manual Lloyds register of shipping (Lloyds, 1907), locations of signal stations in the UK, Australia, South America, West Indies and Bermuda are listed. These stations were used in comparison to the German signal stations, not for weather warnings, but fto comparer weather communication and also ship pessenger communication with the shore. Information about additional meteorological observation at the Lloyd's signal stations are not available.

Signal stations also existed in the USA. Along the east coast, special telegraph lines were supported by the US Army for ship communication in the 1870's. Warning flags were also used at the Great Lakes[1]. At the west coast of the USA, in San Francisco in 1850, two signal stations were built at the Golden Gate to advise the city of the approach of vessels by two arms semaphores that indicate the type of approachig vessels. Also, the dropping of a time ball was done in the exact moment of moon for checking the accurance of ship chronometers (Brownrigg). In China (Hong Kong) and Japan, signal stations with light and flag signals are used these days to navigate vessels in coastal and harbour waters (HKO and Kaiho).

[1]Personal communication by James R. Fleming on 11. January 2016, Professor of Science, Technology, and Society, Colby College Series editor, Palgrave Studies in the History of Science and Technology.

1.1.3 Data Rescue

The rescue of historical handwritten data has a high relevance for climate research. The transformation of historical data in a digital format ensures this historical data can be incorpotated into current scientific research. There are various international data rescue activities (called DARE) (Allan et al. (2011) and
Brunet and Jones (2011)). The South African Science Service Centre for Climate Change and Adaptive Land Management (SASSCAL) initiative unites Angola, Botswana, Namibia, South Africa, Zambia and Germany. Other initiatives are the International Surface Temperature Initiative (ISTI), Atmosphere Circulation Reconstructions over the Earth (ACRE), International Comprehensive Ocean-Atmosphere Data Set (ICOADS) and the COPERNICUS project, which will use the data for reanalysis-related activities (Kaspar et al., 2015).

1.1.4 Homogeneity

An inhomogeneity is a temporal variability, which does not happen due to meteorological or climatological phenomenons, but because of technical measurement reasons (Conrad and Pollak, 1950). The homogeneity of the time series of observational data is very important for assessing a trend analysis in storminess. Instrumental changes, sampling routines, surrounding environments or changing observers can cause inhomogeneities during the time period (Jones et al., 2007). The Beaufort (Bft) wind observations are especially sensetive to the inhomogeneties caused by the differences in nominal observing time and the stage of development of the waves (Thomas et al., 2005). Current studies of the homogenization of Bft wind observation data are not known. The study of Thomas et al. (2005) shows development of the wind sea state observed by voluntary observing ships in Canadian waters to the Bft-scale.
Further introduction to the homogenization of observation SLP data is given in chapter 3.

1.2 Reanalysis Data

Several reanalyses exist and are used for studies in long-term trend analysis of storminess. The reanalyses datasets, which are most frequently used in studies of long-term trend analysis in storminess are listed in table 1.1. The ERA-40 and ERA-Interim reanalyses are beeing developed by the European Centre for Medium-Range Weather Forecast (ECWMF). The ERA-Interim reanalysis was conducted in part to prepare a new atmospheric reanalysis, replacing the ERA-40 reanalysis (Uppala et al., 2005), extended back to the early part of the 20th century (Dee et al., 2011). The analysis of atmospheric near surface fields over the North Sea with hindcast simulations, forced by the ERA-40 reanalyses, is demonstrated in Bülow et al. (2013). In relation to storminess Smits et al. (2005) uses ECMWF reanalysis data for the evaluation of storminess in the Netherlands. The NCEP/NCAR reanalysis is a global reanalysis with atmospherical data going back to 1948 (Kalnay et al., 1996). The estimation of storm trends in Northern Europe of NCEP/NCAR reanalysis data can be found in Smits et al. (2005). The Twentieth Century Reanalysis (20CR) is beeing developed at the National Oceanic and Atmospheric Administration (NOAA) and assimilates, additional to the sea ice and sea surface temperature, the SLP data. The 20CR reanalysis is the longest global reanalysis dataset going back to 1871 (Compo et al., 2011). Long-term trends in storminess, derived by the 20CR reanalyses dataset for the northeast Atlantic, is examined by Krüger and von Storch (2012) and for North Europe by Wang et al. (2013a). The study by Krüger and von Storch (2012) shows inconsistencies between long-term trends in storminess derived from the 20CR reanalysis and observations. The results are discussed in Wang et al. (2013b).

Table 1.1.: Common atmospheric reanalyses used for long-term trend analysis in storminess. Denoted are the name, the time period, the resolution, the coverage and the institute.

ERA-40	1957-2002	125 km×125 km	Global	ECMWF
ERA-Interim	1979-present	79 km×79 km	Global	ECMWF
NCEP/NCAR	1948-present	2.5°× 2.5°	Global	NCEP/NCAR
20CR	1871-2012	210 km×210 km	Global	NOAA

1.3 Geostrophic Wind

The geostrophic wind is defined as the theoretical wind that is the balance between the coriolis effect and the pressure gradient force. The geostrophic wind blows parallel to the isobars and is given by

$$v_g = \frac{1}{\rho f} k \times \bigtriangledown p \tag{1.1}$$

with the air density ρ, the coriolis parameter f, the vertical unit vector k and the gradient of air pressure $\bigtriangledown$ p (Etling, 2008).

The Geostrophic Wind as a Wind Proxy
The geostrophic wind can be derived from triangles of SLP data. This method was firstly used for the long-term trend analysis of storminess in the German Bight by Schmidt and von Storch (1993). Three different time series are needed to derive the geostrophic wind within a triangle, independent from observations within the triangle. The calculation of the geostrophic wind is described in Krüger et al. (2013). Details of the method are also given in Schmith (1995) and Wang et al. (2009).
Studies on the variation of the geostrophic wind in the German Bight, derived from triangles, were first done by Heiner Schmidt from the DWD (Schmidt, 1991). Further investigations in the evaluation of long-term trends of the geostrophic wind in the German Bight are shown by Schmidt and von Storch (1993). The relationship between surface wind and the geostrophic wind in the German Bight was first published in Luthardt and Hasse (1981). The relationship between the pressure field and the surface wind in the German Bight was published by Luthardt and Hasse (1983). Krüger and von Storch (2011) show the evaluation of the geostrophic wind as a proxy for storm activity by using reanalysis data.

1.4 Thesis Objectives

This thesis is part of the Excellencecluster Integrated Climate System Analysis and Prediction (CliSAP), which is founded by the Deutsche Forschungs Gesellschaft (DFG). The first phase of CliSAP took place from 2007 to 2012 and the second phase CliSAP2 is running from 2012 to 2017. The CliSAP

is a collaboration of the University of Hamburg, the Max-Planck-Institute for Meteorology, the Helmholtz Zentrum Geesthacht (HZG), the Deutsches Klimarechenzentrum (DKRZ) and other research institutions. The interdisplinary cluster unites three topics: The dynamics and variability of the climate system, the climate impact and the climate change and social dynamics. This thesis is conducted as part of the CliSAP2 Project and its subproject B4, regional storms and their marine impacts.
The following research questions are part of the aims of this project:

- Are the historical meteorological observation data of signal stations worthwhile for scientific research in regard to the long-term trend analysis of storminess at the German coasts?
- Are the SLP and wind data of signal stations homogeneous in time and space?

1.5 Thesis Outline

The following thesis contains three main chapters. The results of the chapters two to four answer the main research questions. Chapter 2 has been published in Wagner et al. (2016).
Chapter 2 examines the introduction of signal stations, the data of signal stations and a first analysis on the quality of the data in two different ways. A routine quality test is applied on the signal station data and an estimation of two historical storm surges is done.
Chapter 3 is about the homogeneity of the SLP data of signal stations. The SNHT is applied on the SLP data of the signal station, followed by a homogenization of these data.
The evaluation of the wind storminess and SLP data is done in chapter 4. Long-term trends of the geostrophic wind statistics are calculated from the SLP data for three triangles, one in the German Bight and two in the western Baltic Sea. The calculation is done with observational data and reanalysis data from 1967 to 2012. SYNOP-data, as well as observational data are used, instead of the signal station data, because of the unavailability of matching time periods for the signal station SLP data with the reanalysis data. In a second step, the wind observation data from signal stations are analyzed over a time period of 120 years.

2 Signal Station Data along the German Bight and Southern Baltic Sea Coast

In the archive of the marine weather office of the DWD in Hamburg (Kaspar et al., 2015), there are numerous historical handwritten weather observation journals, which contain almost unnoticed original observation sheets, of stations along the German Bight and the southern Baltic Sea coast. The so-called signal stations were positioned close to the coastline in Denmark, Germany, Poland, Russia and Lithuania to facilitate the issuance of storm warnings for the coastal population and mariners by hoisting optical signals in the form of barrels and cones. In addition to providing a warning, meteorological observations were done to validate the alerts.
In this chapter the history of the signal stations is described and an overview on the measured data and the data quality is given.

2.1 History of Signal Stations

The signal stations were set up to communicate warnings issued by the Deutsche Seewarte (German Naval Observatory). The Deutsche Seewarte was established in 1875 and existed until the end of Second World War (WWII) in 1945. From 1945 to 1999, the warnings by signal stations were issued by the naval department (colloquially called 'Seewetteramt') of the DWD. Information about the signal stations and also the instructions for operating the warnings are documented in reports published by the Deutsche Seewarte between 1876 and 1938 (Seewarte (1876), Seewarte (1880), Seewarte (1889) and Seewarte (1902), Seewarte (1938)). After WWII, two further documentations were published by the Seewetteramt in 1955 and 1969 (DWD (1955) and DWD (1969)).
In 1982 all hand-operated signal stations were closed and the hourly warnings were actually done by radio broadcasting (Wulff, 1982). A signal station consists of a mast with a height of about 20 m, complete with ballons, triangles, cones and flags. Fig. 2.1 shows two signal stations with its masts and a detailed drawing of a signal station mast which is documented at the reports

Figure 2.1.: On the left side, a picture of the signal mast in Greetsiel and in the center the signal mast in Karkeln (Poland) before 1945 with optical signals. On the right side, a detailed drawing of a signal mast with optical signals. Source: DWD.

of the Deutsche Seewarte (Seewarte, 1938). On the left side, the signal station in Greetsiel at the coast of the German Bight (recorded in 2012) and in the center the signal station in Karkeln (now Poland) before 1945 (the exact date is unknown) is pictured. The detailed drawing (right side) shows two flags on the left side and a triangle and a ball on the right side. The two flags indicate the changing directions of the wind and the combination of a barrel and a cone on the right side of the mast indicate the warning of a severe storm with a wind force of 10 to 12 Bft. A single ball announces a warning of an atmospheric disturbance, which maybe leads to stormy winds with a wind force of 6 to 7 Bft. The details could be gleaned from the telegram at a displayed case. A raised triangle shows the expectation of a storm on the same or the next day. The triangles are visible from each geographic direction as one dark triangle. Two triangles indicate the direction of the storm from the East and only one triangle indicates a storm direction from the West. The combination of two triangles with its peaks up or down indicate the direction of a storm from the North or the South (Seewarte, 1876).
Until the beginning of the 20th century, different classes of signal stations were operated. First class signal stations reported wind force and wind direction. The warning was expressed by hoisting a combination of barrels and cones. Furthermore, the expected change of wind direction was given by flags. At second class signal stations braided balls were hoisted for warnings.

Figure 2.2.: Positions of all 164 signal stations with weather observations from 1877 to 1999 along the coastline of the German Bight and the southern Baltic Sea. Not all stations existed during the same time period.

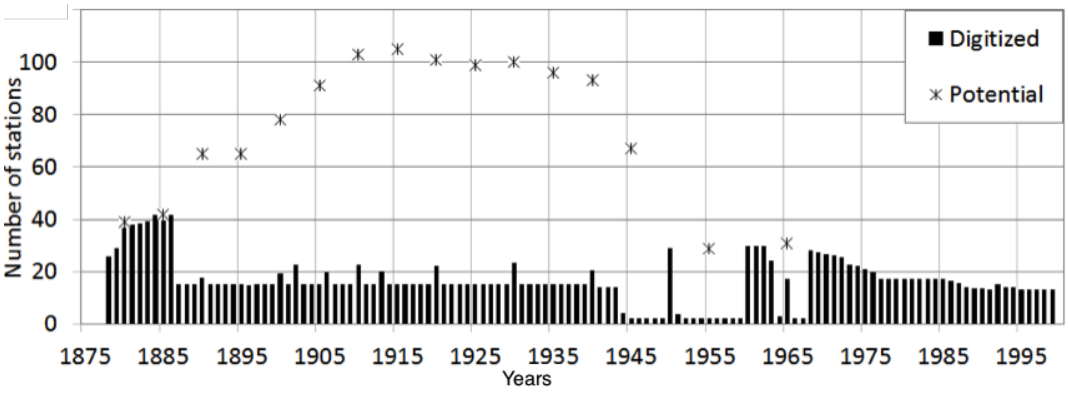

Figure 2.3.: Distribution of numbers of signal stations and digitized data during the time period from 1875 to 1999. The bars show the digitized data and the asterisks the total number of available reports all five years. Not all have been digitized so far.

Since 1882, night signals were set at some signal stations and a red light warned of a storm. Since 1912, a combination of white and red lights warned of a strong storm. A green light indicated strong wind. However, the diversity of a combination of optical signals for storm warning was a common method in the early 20th century.

For the verification of the storm warnings meteorological observations and measurements were done by workmen at the signal stations. The observations were done typically three times a day (8, 14 and 20 Central European Time (CET)). Once a month, observation data sheets were sent back to the Deutsche Seewarte in Hamburg, where annual journals of the data were prepared. These data did not enter the synoptic analysis nor synoptic maps of the

weather service, the data represents a database, which is completely independent of routine historical weather maps. The data were not used for weather analysis or forecasts. They complement the conventional data archive. The details of these data are described in chapter 2.2.
Altogether, 164 signal stations were set up along the German Bight and southern Baltic Sea coast. In addition, some stations operated on light ships, which were stationed in the coastal sea. Fig. 2.2 shows the positions of all signal stations in the period from 1877 to 1999: Their positions ranged at the German Bight from Borkum to Sylt and at the southern Baltic Sea from Aarosund (now Denmark) to Palanga (now Lithuania). A table of all signal stations is given in Fig. A.1, Fig. A.2, Fig. A.3 and Fig. A.4. In 1877 41 signal stations were built. The number of active signal stations changed during the time period. In 1945, after WWII, the number decreased from a maximum in 1909 of 102 working stations to 30 stations. In 1999 the last 13 stations were closed. Fig. 2.3 shows the distribution of numbers of signal stations and digitized data during the time period from 1875 to 1999. The bars show the digitized data and the asterisks the total number of available reports for all five years. Not all data sheets have been digitized so far. The greatest potential is given from 1885 to 1945 with up to 105 stations providing data (more information at DWD (2016b)). Finally, a creation of time series for different lengths of time periods of meteorological data from a multiplicity of data along the coastline of the German Bight and southern Baltic Sea is possible.

2.2 Data of Signal Stations

The archive of signal stations contains about 800 handwritten journals with wind and weather observation data. Fig. 2.4 shows a scan of an original journal sheet. It shows the observed data of the first five days of January in 1910 of Dornbusch station at the Baltic Sea Coast. The seven rows contain the following meteorological information from left to right: Date, SLP, wind direction and wind force, weather conditions, sea state, precipitation and weather remarks. The data has begun to be manually digitized since 2010 for allowing possible comprehensive scientific analysis. At present about 30 % of the data are digitized (see Fig. 2.3). The scanning of the original sheets to protect the handwritten data from physical decomposition is planned and will begin at the end of 2016.

Table 2.1.: List of all observed variables with unit, report time (CET), time period and number of years with observation.

Element	Unit	Report Time CET	Time Period	Years
Sea level pressure	mmHg	8	1877-1939	63
Wind direction	8,16,32 sections	8, 14, 20	1877-1999	123
Wind force	Bft	8, 14, 20	1877-1999	123
Weather condition	0 - 9	8, 14, 20	1877-1999	123
Visibility	0 - 9	8, 14, 20	1877-1999	123
Sea state	0 - 9	8, 14, 20	1838-1999	62
Precipitation height	mm	8, 20, (24h)	1838-1999	62
Weather trend	Significant events	irregularly	1877-1999	123

All records contain values of estimated wind force and direction, as well as weather conditions and visibility. Additionally, prior to 1940, SLP, precipitation and in some cases the sea state have been recorded (Tab. 2.1). All stations reported three times per day (08, 14 and 20 CET). In case of storm warnings the frequency of SLP measurements was increased irregularly. There are nine time series with data covering more than 100 years. All in all, there are 44 time series longer than 60 years and the time series of Travemünde station comprises wind data of 125 years.

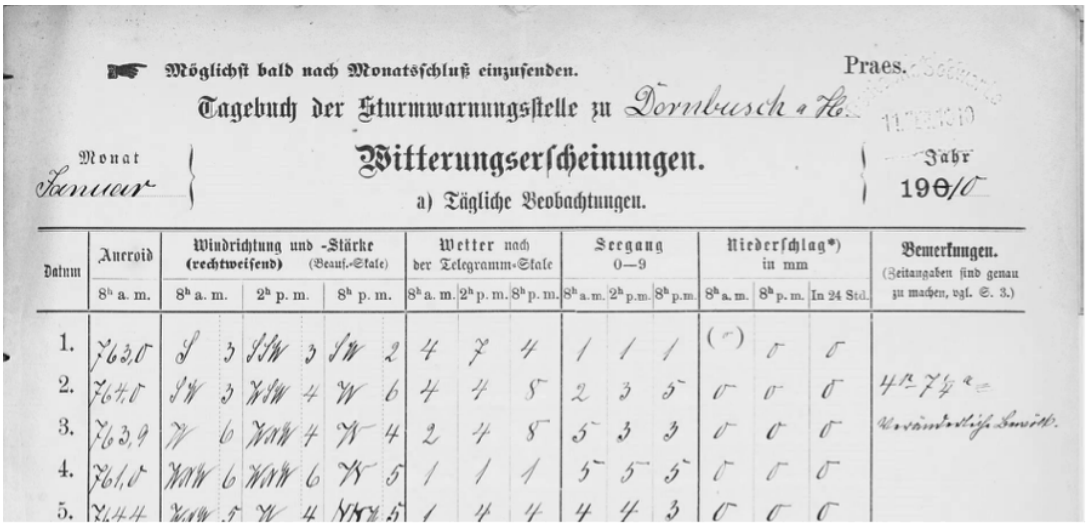
Möglichst bald nach Monatsschluß einzusenden. Praes.

Tagebuch der Sturmwarnungsstelle zu Dornbusch a/O.

Monat Januar — Witterungserscheinungen. — Jahr 1910

a) Tägliche Beobachtungen.

Datum	Aneroid	Windrichtung und -Stärke (rechtweisend) (Beauf.-Skale)			Wetter nach der Telegramm-Skale			Seegang 0—9			Niederschlag*) in mm			Bemerkungen. (Zeitangaben sind genau zu machen, vgl. S. 3.)
	8h a. m.	8h a. m.	2h p. m.	8h p. m.	8h a. m.	2h p. m.	8h p. m.	8h a. m.	2h p. m.	8h p. m.	8h a. m.	8h p. m.	In 24 Std.	
1.	763,0	S 3	SSW 3	SW 2	4	7	4	1	1	1	(—)	0	0	
2.	764,0	SW 3	WSW 4	W 6	4	4	8	2	3	5	0	0	0	
3.	763,9	W 6	WNW 4	W 4	2	4	8	5	3	3	0	0	0	
4.	761,0	WNW 6	WNW 6	W 5	1	1	1	5	5	5	0	0	0	
5.	764,4	WNW 5	W 4	NNW 5	1	4	4	4	4	3	0	0	0	

Figure 2.4.: Scan of an original sheet from a journal of Dornbusch station in January 1910. The seven rows contain the following meteorological information from left to right: Date, SLP, wind direction and wind force, weather conditions, sea state, precipitation and weather remarks.

The instructions for how to observe the different meteorological data and

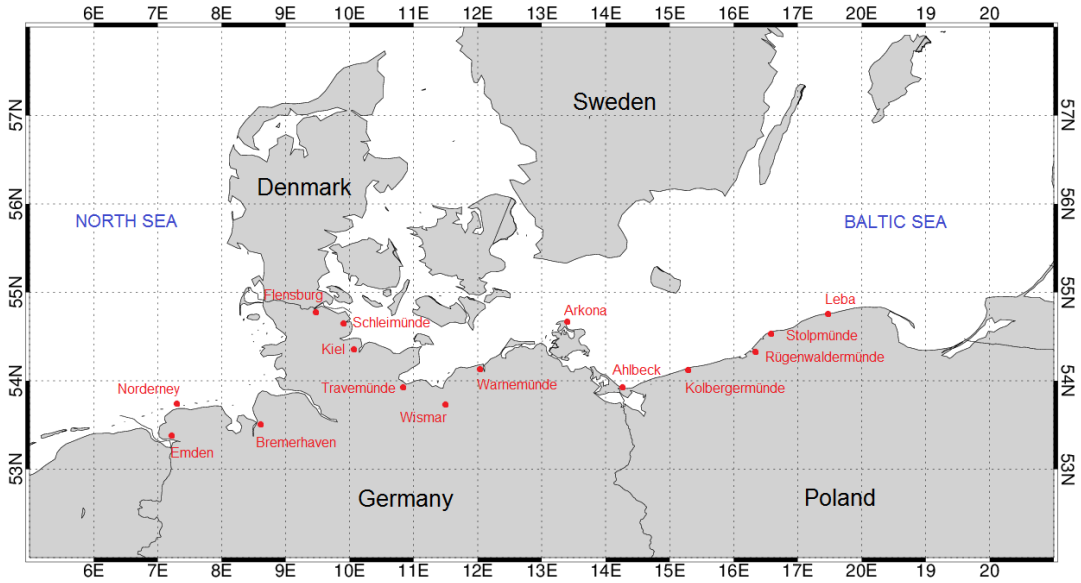

Figure 2.5.: Positions of 15 selected and primarily digitized signal stations along the coastline of the German Bight and the southern Baltic Sea.

how the observation rules changed during the time, are written in the observation instructions of the Deutsche Seewarte in Seewarte (1876) and DWD (1969). The rules to prepare the measuring instruments and to metering the data are documented. Also, the encoding of weather keys was noted. The SLP was measured in mmHg and the reduction to Normal Height Null (NHN) was done by an increase of 1 mmHg each 10 m above sea level (a.s.l.). The wind direction was, most of the time, recorded in terms of the 16-parts wind rose (temporary 8-partly or 32-partly). Since 1902, the wind direction of 00 was used at calms and the denotation of "East" was abbreviated since 1925 with "O" (as in the German term "Osten"). The wind force was estimated by the movement of the surrounding nature, such as the movement of the trees and the sea state. The wind force was stated in the Bft-Scala with the wind forces 0-12. The weather observation was noted by a key from 0-9, representing: clear, bright, half dull, cloudy, dull, rain, snow, mist, haze and thunderstorm conditions. Also, the sea state was recorded by a key from 0 to 9, which means: plain, very quiet, quiet, light moved, moderate moved, agitated, high, very high and severe. Same with the visibility: 9 classes ranging from 0 to 9: up to 50 m, 200 m, 500 m, 1 km, 2 km, 4 km, 20 km, 50 km and more than 50 km. The precipitation was measured two times a day in tenth

millimeters (1/10 mm) and additional detailed notes of the weather conditions were also done. Because of this, the observation data from the various signal stations are inconsistent in their measuring methods. These inconsistencies have to be considered in the following studies.

For further estimations and homogenization (Chapter 3), the wind and SLP data of 15 stations along the coastline of the German Bight and the southern Baltic Sea are used. These 15 stations are chosen because of their evenly distribution along the coasts (see Fig. 2.5). These 15 stations were Emden, Norderney and Bremerhaven at the German Bight. Flensburg, Kiel, Wismar, Travemünde, Warnemünde, Arkona, Ahlbeck, Stolpmünde, Rügenwaldermünde, Kolbergermünde and Leba at the Baltic Sea Coast. A description of these data is given in 2.2.

Table 2.2.: List of 15 selected and primarily digitized signal stations along the coastline of the German Bight and the southern Baltic Sea coast with the name, the country in 2016, the geographic coordinates and the height in m.

Station Name	Country	LON	LAT	Height in m
Emden	Germany	N53.93	E7.18	not known
Norderney	Germany	N53.70	E7.15	not known
Bremerhaven	Germany	N53.55	E8.57	not known
Flensburg	Germany	N54.80	E9.43	5
Schleimünde	Germany	N54.67	E10.02	15
Kiel	Germany	N54.40	E10.18	11
Travemünde	Germany	N53.97	E10.88	31
Wismar	Germany	N53.90	E11.47	not known
Warnemünde	Germany	N54.18	E12.08	10
Arkona	Germany	N54.68	E13.43	66
Ahlbeck	Germany	N53.93	E14.18	not known
Rügenwaldermünde/Darłówko	Poland	N54.42	E16.40	not known
Stolpmünde/Ustka	Poland	N54.58	E16.87	12
Kolbergermünde/Kołobrzeg	Poland	N54.18	E15.57	9
Leba/Łeba	Poland	N54.77	E17.55	not known

2.3 Quality of Signal Station Data

The quality of the signal station data is checked in different ways: The first step is to test the data on mistakes, which come along by observation and digitization. Typical mistakes arise by changing the observer or transposed digits during digitization. Different observers could perceive the same weather conditions in different ways. For example, when the wind force was observed by tree or wave movements, that depends partly on personal sensation. But the observation method for wind is not influenced as much by changing cultivation, such as new buildings. Obvious uncertainties can be found by the validation program *validat*, which is described in 2.3.1.
In a second step the capability of using signal station data for storm estimations is examined by analysing case studies of two historical storm surges. This analysis of the storm surges from 1906 and 1913 is described in 2.3.2.
The third step is to examine the long-term homogeneity of the signal station data. This is done in chapter 3.

2.3.1 High Quality Tests by *Validat*

Obvious mistakes can be found by the quality control program *validat*. *Validat* is a operative used routine for automatic quality checks of meteorological data, which was developed by the DWD (Tinz et al., 2015). The word *validat* is a combination of *validation* and *data*. The aim of the *validat* routine is to detect false data. For each detected uncertainty, a byte of quality is given to the concerned value. The original data persists and can be corrected by hand. Fig. 2.6 shows a schematic chart of the validat progress. The inputs (red boxes) of the program are given by the data file, which should be proved, and a configuration file. The output (green boxes) is given by an output-file, which comprises the original data with bytes of quality, a list of the detected uncertainties, a protocol and a file concerning unused massages. In addition to the input-files, *validat* accesses further subroutines, a land-sea-mask and for the climatological tests on the ERA-Interim a reanalysis dataset. The data testing routine for signal station data goes through a sequence of different steps. Firstly, a formal test, secondly, a climatological test and thirdly a repititional test. The formal check is searching for permissible signs in a first step and is proving the data on a given reasonable codomain in a second step. During the

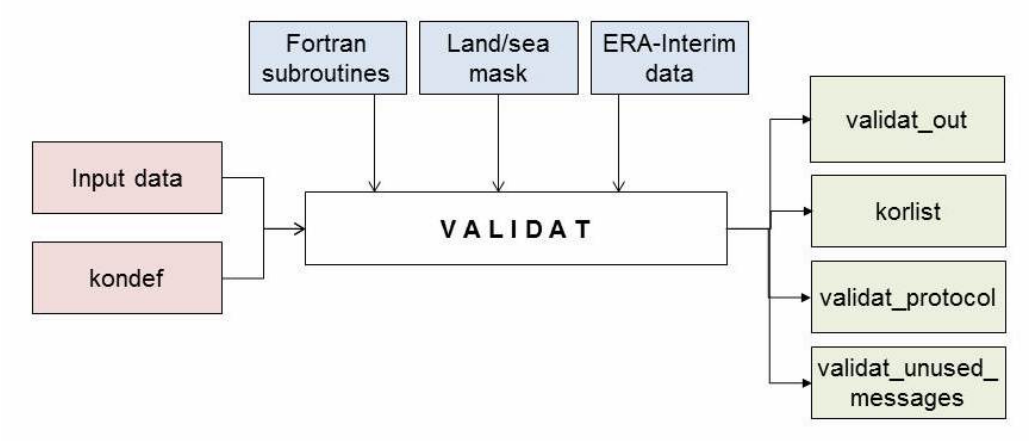

Figure 2.6.: Schematic chart of *validat* progress with input (red) and output (green). The blue boxes display subroutines.

climatological check it is proved, whether the values are within the defined climatological ranges. The threshold values are given by the climatological mean of the ERA-Interim-Reanalysis data base (Dee et al., 2011) (Tinz et al., 2013). The repitition check tested whether any value is unchanging during a defined time period. Therefore, there are two quantitative threshold values. A detailed description of all critical values as an example of a configuration file is given in Fig. A.2.

For the 15 stations the *validat* routine is applied to the SLP, the wind force and wind direction data. The absolute number of formal mistakes during the quality check is shown in Fig. 2.7 (left). The most formal mistakes occur for the SLP data of station Arkona. Also, formal mistakes of date and wind direction occur for ten of fifteen stations. The absolute number of climatological and repititional uncertainties during quality check by *validat* for 15 stations is shown in Fig. 2.7 (right). The most climatological uncertainties occur for the wind force for Warnemünde station. Additional repititional uncertainties for the wind force occur for Kiel station. Formal mistakes such as missing entries or unsuitable marks, like colons or crosses instead of the date, can be a result of the digitization or retyping of the data. A further formal mistake is the entry of '999' to represent a missing data, but *validat* indicates a not matching of the codomain for DD. Accordingly, *validat* by itself causes the formal mistakes for DD data. For SLP data the formal mistakes occur due to missing calculations from mmHg to hPa. Therefore, the SLP values do not match the codomain and *validat* gives a formal uncertainty. The missing cal-

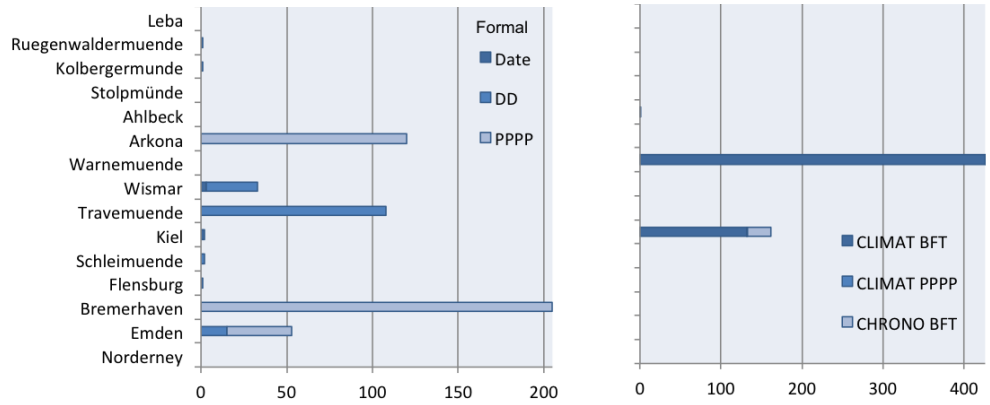

Figure 2.7.: Absolute number of formal mistakes (left) during quality check by validat for 15 signal stations. The most formal mistakes occur for the SLP data of station Arkona. Also formal mistakes of date and wind direction occur for ten of 15 stations. Absolute number of climatological and repititional uncertainties (right) during quality tests by *validat* for 15 stations. The most climatological uncertainties occur for the wind force for the station Warnemünde. Additional repetitional uncertainties for the wind force occur for station Kiel.

culation from mmHg to hPa occurs with a retyping process after digitization and before *validat*.

2.3.2 Two Storms in 1906 and 1913

In the following two case studies two storms, associated with significant surges, are analyzed using the signal station data. The first case study is a storm in 1906 at the coast of the German Bight and the second is the storm in 1913, which occurred in the region of Rügen and Usedom in the southern Baltic Sea. The data are all quality-controlled by *validat*.
Additional to the signal station data, other data are used for the analysis of these storms and their surges. Firstly, synoptic maps of the weather forecast from the Imperial Navy (Kaiserliche Marine 1906, 1913) are used. The maps include isobars, wind force and wind direction information over Europe. Secondly, the sea level data of the Water Level Office of the BSH of the station Greifswalder Oie are used.

Storm Surge 1906
The storm surge on the 12 March in 1906, which occurred in the German

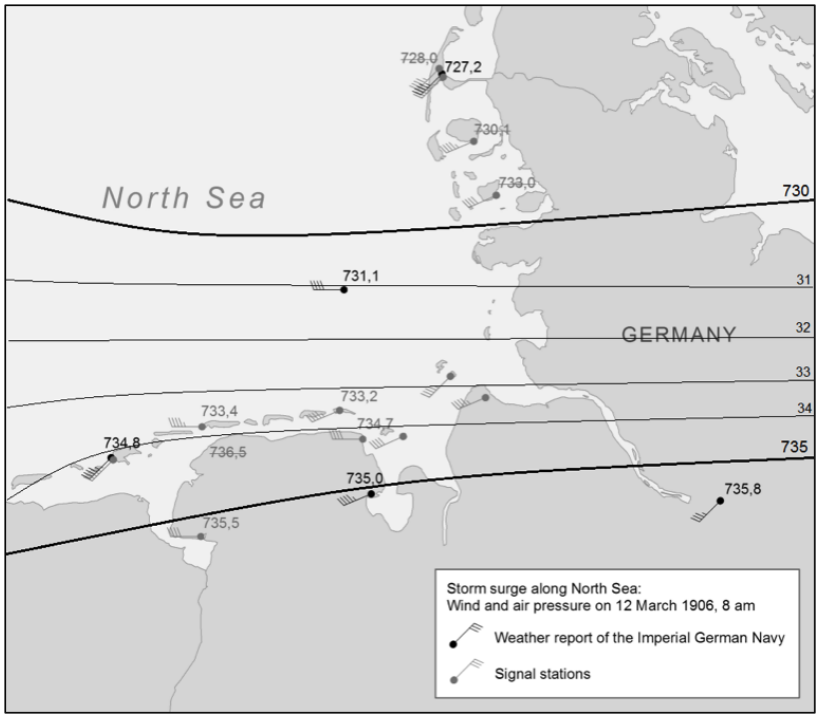

Figure 2.8.: Wind direction and wind force with air pressure data on 12 March in 1906. The black flags represent the data of the Deutsche Seewarte and the grey ones represent the data of signal stations. The black lines represent the isobars of the weather report and the thin grey lines represent the isobars based on the signal station data. The crossed SLP data are disregarded for the isobars depending on signal stations.

Bight, offers the highest known water level ever in this region with a water level of 3.62 m a.s.l. (uncertain source). In Fig. 2.8 the wind observations are illustrated. The black vanes represent the wind observation and SLP measurements of the six weather stations of the Deutsche Seewarte. The grey vanes represent the newly digitized data of 14 signal stations. The signal station data nearly tripled the monitoring network at the coast. The streaks and triangles at the vanes display wind forces up to 10 Bft, which indicates a severe storm. The wind directions and wind forces, reported by the signal stations, are consistent with the six weather station data.

The synoptic situation on 12 March 1906 is shown on the weather map of the Deutsche Seewarte on the left Fig. 2.9. This weather map was created on the basis of the weather report data and the station data have not entered this historical map. A low-pressure area was located in the north of Denmark. A low-pressure area over the south of Norway leads to strongly crowded

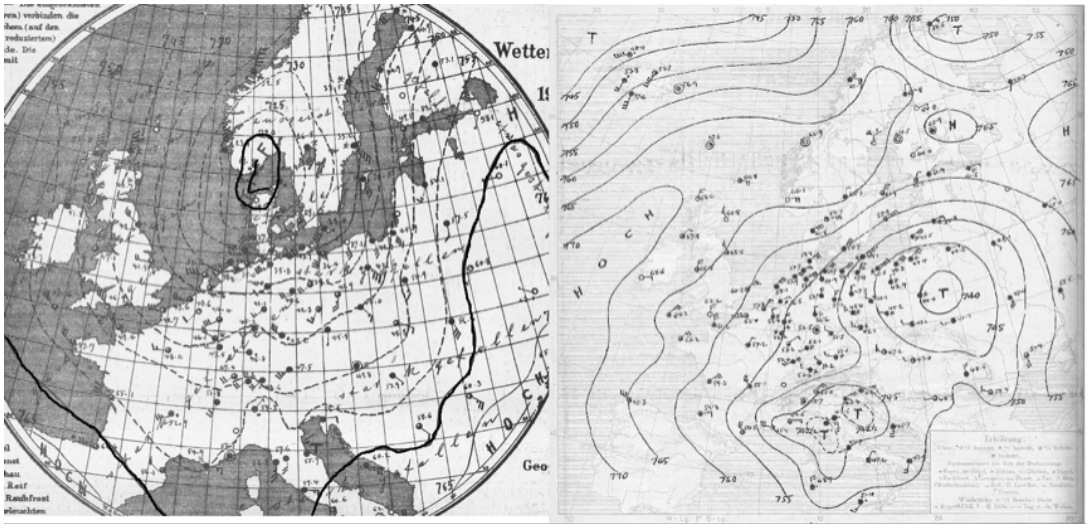

Figure 2.9.: On the left side the synoptic situation on 12 March 1906 over Europe and on the right side the synoptic situation on 30 December 1913. Both weather maps are based on the observation data of the daily weather report of the Deutsche Seewarte.

isobars in the German Bight region with a spin from the West to the East. Moreover, the dominant wind direction of the signal station data, as well as the routine observations, is westerly.

The SLP data of the signal stations (Fig. 2.8) allow us to add isobars in a resolution of 1 mmHg to the original 5 mmHg isobars of the weather report in the southern German Bight. The black lines show the original isobars belonging to the five stations of the Imperial German Navy and the grey lines the isobars based on signal station data, which extend the network from five to thirteen stations. The crossed SLP data are not considered for the isobars depending on signal station data. These SLP data do not match the pressure field exactly. Thus, the crossed SLP data are not rated as wrong, but as not plausible. The reasons for not matching the air pressure field of the crossed data, especially for the three crossed SLP data at the west coast of Germany, could be the assumption that the isobars by the Imperial German Navy are nearer to the truth, but it could also be the other way round. However, there is as yet a sufficient number of data for getting a higher resolution of isobars.

Fig. 2.10 shows the course of the SLP and the observed wind force during 9 to 14 March 1906 at the Borkum station. The circles stand for the available standard observations of wind force and SLP two times a day and the dots

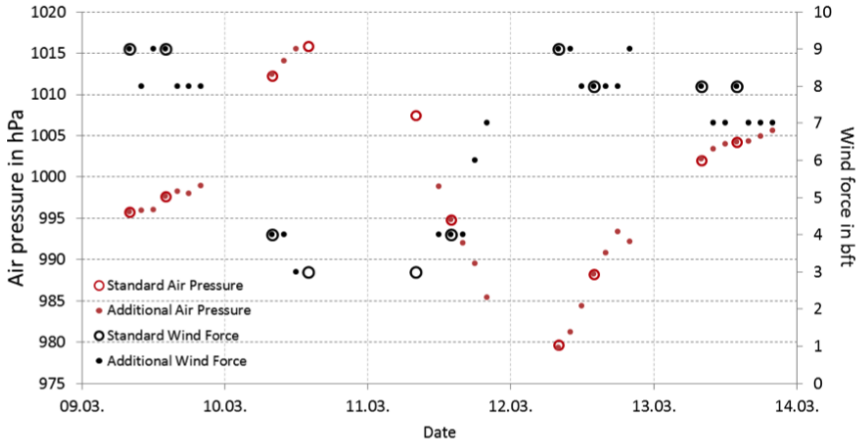

Figure 2.10.: Distribution of air pressure and wind force at Borkum station. The circles display the routine observations and the dots display the additional observations during storm surges.

for additional wind and SLP observations during stormy days. The course of the SLP and wind force data during this time period is antidromic. Therefore, a more detailed course of events can be described by adding the observation signal station data during stormy days.

Storm Surge 1913

The storm surge, which occurred on 31 December 1913, caused serious damage to the landscape and infrastructure in the region of Rügen and Usedom (von Storch et al., 2015). This storm surge was among the highest reported water levels with 2.30 m a.s.l. in this region, having been exceeded only by the storm surges in 1872 and 1904 (Rosenhagen and Bork, 2009).

Fig. 2.11 shows the wind observation on 30 December in 1913 at the southern Baltic Sea coast. All in all, wind data of 73 signal stations along the Baltic Sea coast could be added. The seven black vanes display the data of the daily weather report at eight stations of the Deutsche Seewarte (1913) and the grey ones the signal station data. The dominant wind direction on 30 December 1913 at all 73 signal stations along the southern Baltic Sea coast is north-easterly. The strongest observed wind force is 11 Bft. The synoptic situation on 30 December 1913 is shown on the weather map in the right Fig. 2.9. This weather map was created on the basis of the weather report data and shows the isobars, wind force and direction with a low-pressure area over southern Poland. Fig. 2.11(b) shows the German part of the Baltic Sea Coast. The black lines represent the isobars of the weather report maps. The signal

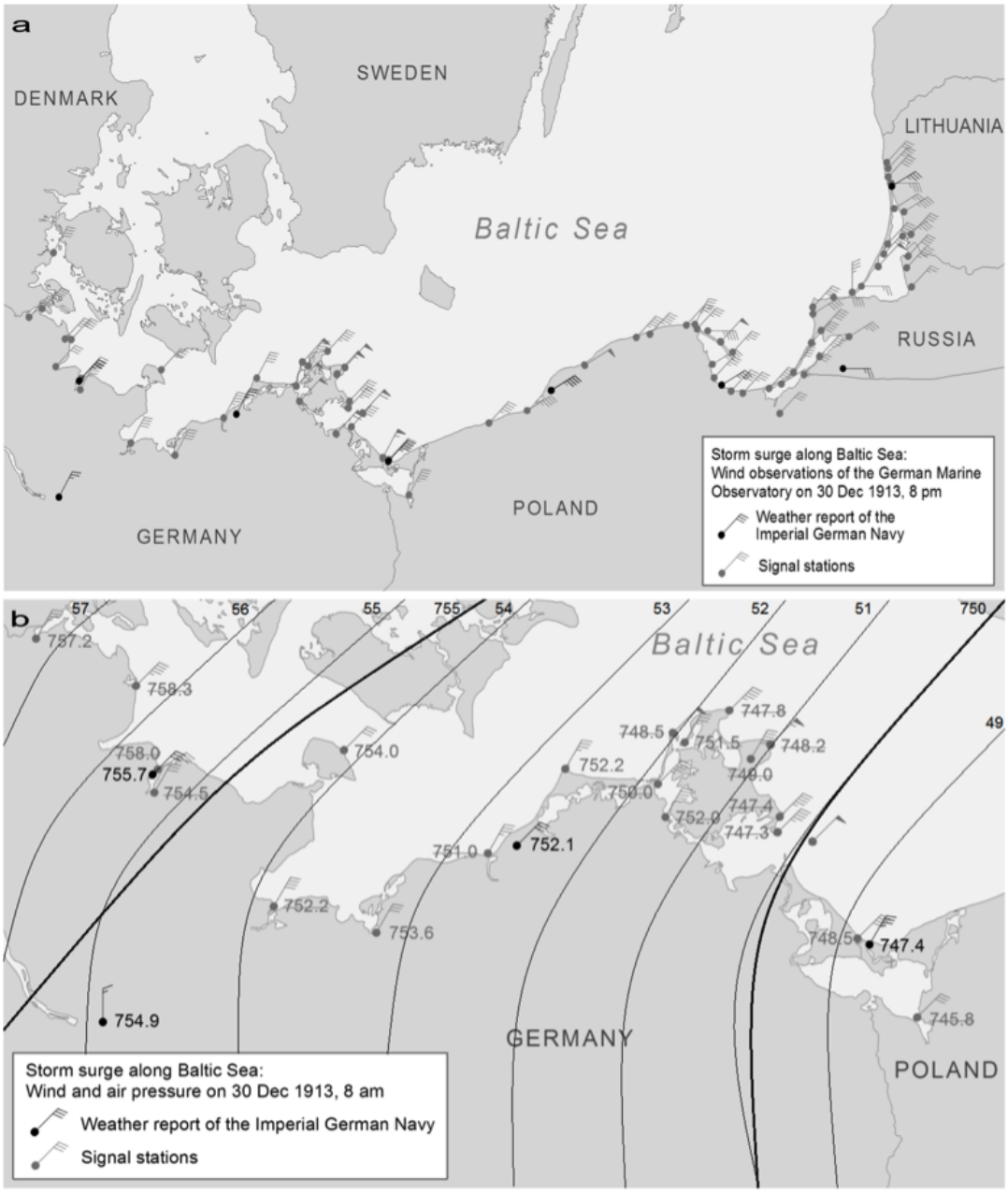

Figure 2.11.: (a): Positions and wind observations of the signal stations reported on 30 December 1913. The black flags represent data of the Deutsche Seewarte and the grey ones represent the data of signal stations. (b): The German part of the Baltic Sea coast with wind and air pressure information. The crossed SLP values are unaccounted for the isobars. The black lines represent the original isobars by the weather report and the grey lines represent the isobars based on the signal station data.

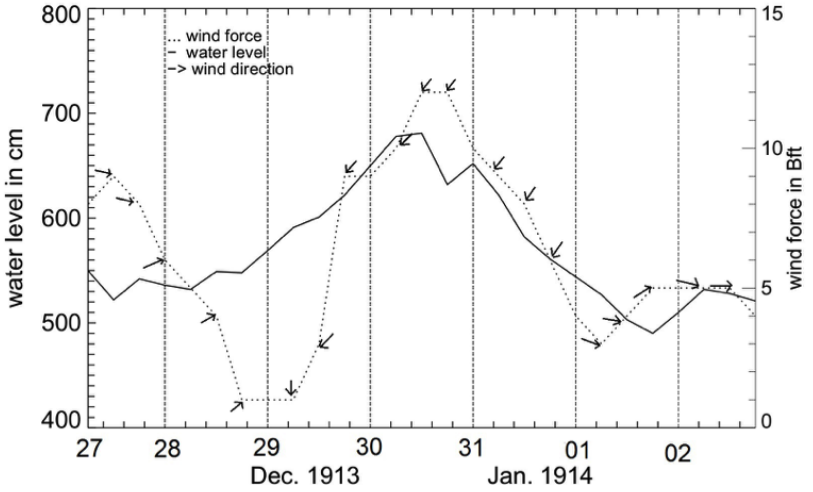

Figure 2.12.: Chronological sequences of water level, SLP, wind force and direction at Greifswalder Oie in the period from 27 December 2013 to 2 January 1914.

station data allow a more detailed analysis, with a higher resolution, of the isobars in the Rügen region, where the storm surge mainly occurred. The crossed SLP data are chosen with the same principle as in Fig. 2.11.

The maritime meteorological data of 27 December 1913 to 2 January 1914 are shown in Fig. 2.12 for the station Greifswalder Oie. The course of the wind force is shown by the dotted line and the course of the water level in cm is shown by the solid line. The wind direction is given by the arrows. Consistently, the water level rose up to 1.8 m a.s.l. on 30 December 1913 at this station and the wind force grew to a maximum of 12 Bft on 30 December 2013 after a minimum of 1 Bft. The wind direction changed from South-West to North-East on 29 December 2013. This course of data describes the passage of a low-pressure area on 29 December 1913. The chronological sequence of wind direction and wind force at Greifswald Oie confirms also the movement of the low-pressure area.

The additional value of the signal station data is the expansion of the monitoring network in space during the examined storm surges. The wind data, wind force and direction are shown in the spatial analysis as a homogeneous field. The SLP data can be used for a higher resolution of the air pressure field during the analyzed storm surges.

2.4 Summary and Conclusion

There is a new dataset of historical meteorological observation data from 1877 to 1999 of 164 stations. These data were observed at signal stations along the coastline of the German Bight and the southern Baltic Sea. The observed values are SLP, wind force, wind direction, weather condition, sea state, visibility, precipitation and the weather-trend. Because digitisation of the data is not yet complete, the SLP and wind data are first estimated for their quality. The aim is to show the usefulness of this data related to their quality for scientific research. Accordingly, the quality of these data is checked in two ways. Firstly, the testing of the data quality by the routine *validat* on formal uncertainties and secondly, the capability of using signal station data for storm estimations is checked by analysing case studies of two historical storm surges. The first quality test, which is done for 15 selected stations, shows that formal mistakes occur irregularly, but not for all stations and values in the same intensity. Data especially from four stations shows a relative high number of mistakes. Climatological and repititional uncertainties occur in the data of two stations for different values. The maximal number of formal mistakes is only 0.1 % of the checked data. The climatological uncertainty developed to the maximum of 0.3 %. Only the repetitional uncertainty topped out at a maximum of 3 %.
The relatively high percentage value of the repetitional mistakes goes along with the kind of observation in history and is not considered in the following steps of the evaluation of the data. In the second part it was shown that the signal station wind data at the German Bight region and the southern Baltic Sea are well suited for the analysis of extreme wind events. Furthermore, the air pressure data is useful for analyzing the air pressure situation during this extreme event with the base on the storm surges in 1906 and 1913 along the German Bight coastline and the southern Baltic Sea.
In the next chapter the homogenization of the signal station data, as an additional part of quality, is tested.

3 Homogeneity of Air Pressure Data from Signal Stations

The homogeneity of 15 series of SLP data is assessed using the SNHT method described in Alexandersson (1986).
The inhomogeneity or non-homogeneity is an important anomaly of climatologic time series. Changes in measurement instruments, the dislocation of measuring stations, problems with instrumentation, new observer changes in time of observation and changes in the surrounding of a station (e.g. growing of trees, etc.) can lead to inhomogeneities (Schönwiese, 2008).
Two different methodologies for homogeneity testing are in use. Firstly, the direct methodololologies and secondly, the indirect methodologies.
The direct methodologies for testing a time series on inhomogeneities are the use of metadata, a side by side comparison of instruments and statistical studies of instrument changes (Peterson et al., 1998). Metadata of instrument changes and so on can found in meteorological yearbooks or their equivalents. For the signal station data, no metadata of information about changes in instruments or the moving of stations are available. Therefore, information about instrument comparisons or studies about instrumental changes are not allocateable. But in Seewarte (1876) it is written that aneorid barometers were used already from the beginning of measurement at the signal stations.
Indirect methodololologies for homogeneity testing are the use of single station data, the development of reference time series, subjective methods and objective methods (Peterson et al., 1998).
There are different methods to detect and adjust inhomogeneity in time series (Easterling and Peterson, 1992). As a proven standard the SNHT method is described in many different publications and is here used as an objective method. The method is simple and the best known and most widely applied homogenization method (Domonkos et al., 2012) and is also used as standard at the DWD. The methodology of SNHT is described in 3.1. Further methods are described in Ribeiro et al. (2015).
However, in practice it is very difficult to find a station which is homogeneous. So Conrad and Pollak (1950) write about the relative homogeneity of a series. The word homogenous is here used to mean it is relatively homoge-

nous. The discontinuities of the time series can be caused by station relocations or changes in observation procedures.
The inhomogeneities of SLP data, especially in this part of SLP data from signal stations, are presumably caused mostly by changes to the instrumental height, which is related to a station relocation. Also, changes in the procedure of the reduction of pressure to mean sea level is a given factor.

3.1 Standard Normal Homogeneity Test

With the SNHT it is possible to detect shifts in a candidate series, when it is compared with a reference series. The SNHT is applied on the difference series *q*, which is calculated from the difference of the candidate series and the reference series. The method is testing the standardized time series z with the standard deviation S_q of q_i and $\overline{q}$, the mean of q_i

$$z_{\mathrm{i}} = \frac{q_{\mathrm{i}} - \overline{q}}{S_{\mathrm{q}}}. \tag{3.1}$$

Formally, a single shift of the mean level at the candidate series can be expressed as a contradiction to a null hypothesis (H_0) and a consistency to an alternative hypothesis (H_1) as

$$H_0 : z_i \in N(0,1)\ i \in \{1, ..., n\} \tag{3.2}$$

and

$$H_1 : \begin{cases} z_1 \in N(\mu_1, 1) & i \in \{1, ..., a\} \\ z_2 \in N(\mu_2, 1) & i \in \{a+1, ..., n\} \end{cases} \tag{3.3}$$

where N denotes the normal distribution with its parameters, the time unit index *i*, the total number of values in a time series *n* and the last year before a possible shift *a*. H_0 is the ideal case of a homogeneous candidate time series. H_1 says that at some unknown time the mean value changes abruptly (Alexandersson and Moberg, 1997). The intrinsic asymmetry of a statistical hypothesis test is given. The non-rejection of H_0 is not an acceptance or a rejection of H_1, but an rejection of H_0 gives an acceptance of H_1. Based on both

of the hypothesis the test value is

$$T_{\max} = \max_{1 \le a \le n} \{T_a\} = \max_{1 \le a \le n} [a(Z_2)^2 + (n-a)Z_1)^2] \tag{3.4}$$

with the cummulative sums

$$Z_1(a) = \frac{1}{a} \sum_{i=1}^{n} z_i \tag{3.5}$$

and

$$Z_2(a) = -\frac{1}{n-a} \sum_{i=a+1}^{n} z_i. \tag{3.6}$$

Accordingly, the time point of the beginning of a inhomogeneity is

$$a_0 = (a \in T_a = max). \tag{3.7}$$

For a homogeneous time series, any part of the series is normally distributed with $\overline{q} = 0$ and $S_q = 1$. The time series includes an inhomogeneity at the end of the year a, when the data of the first a-years has a mean value equal $\overline{z_1}$ and the $(n-a)$-last years has a mean value $\overline{z_2}$. The standard deviation of both parts is 1. If T is greater than a critical value for the 95 % significant level, which depends on the total number of values n, the null hypothesis of homogeneity can be rejected. Because it is not possible to know the exact distribution of the test statistic of H_0, the simulation of critical levels is necessary. Therefore, large sets of random numbers are used. Typically $2x10^6$ standard normal random numbers are used to simulate critical levels for $n = 100$, which is giving 20 000 series. To obtain a mean value of exactly zero and a standard deviation of exactly one, a standardization of each series is executed. Then the lowest value of the five per cent largest test statistic values, derived from the 20 000 series, is an estimate of the T_{95} critical value (Alexandersson and Moberg, 1997).
Slonosky et al. (1999) and Heinkelmann et al. (2005) show that the SNHT also works for SLP data and it was also shown that the method also works for more than one shift (Heinkelmann et al., 2005). The SNHT method also detected trend inhomogeneities (Slonosky et al., 1999). For the following appli-

cation of SNHT the time series is only analyzed on shift non-homogeneities.

3.2 Inhomogeneity of Signal Station SLP data

For the detection of discontinuities in the time series of SLP data, 15 signal stations along the German Bight and the southern Batlic Sea coast were chosen. These 15 stations, described in 2.3.1, were digitized first. The SNHT procedure requires a homogeneous reference time series. In the literature, the reference series is often taken from reanalysis or model data like in Slonosky et al. (1999). The grid resolution of this reanalysis data from surges such as the UK Meteorological Office SLP dataset, of 5° x 10° is too low for the signal station data, which were located especially in the longitude with a resolution of 1°. Therefore, for the following SNHT for all 15 SLP time series the reference series is created as a mean from three stations. For these five boxes the SNHT is done for three stations each, which created the base for the mean and, consequently for the reference series, for each time series at the given box. The boxes with their belonging stations are shown in Fig. 3.1. For detecting discontinuities the time series, the yearly mean of the SLP data is calculated. The application of the SNHT on yearly mean SLP data of the candidate station was also done in Alexandersson and Moberg (1997) and Alexandersson (1986) for temperature and precipitation data time series. The time series of the yearly mean of the 15 signal stations, with the spatial mean of three stations, each are shown for the boxes 1 to 3 in Fig. 3.2 and for the boxes 4 and 5 in Fig. 3.3. The time series of box 1 with the time series of the yearly mean SLP data of Emden, Norderney and Bremerhaven and the spatial mean of these three stations shows a noticeable peak for Emden station during the time period of 1931 to 1936, which also influences the spatial mean and therefore the reference series considerably. Also, the data of Schleimünde station at box number 2 (Fig. 3.2 middle) shows a noteworthy peak in 1927. Another peak in 1937 is given for all stations in box 2. The other boxes show no noteworthy peaks of one single time series. The station Rügenwaldermünde at box 5 in Fig. 3.3 bottom reveals a gap in 1919. For this year data of several months are not available.

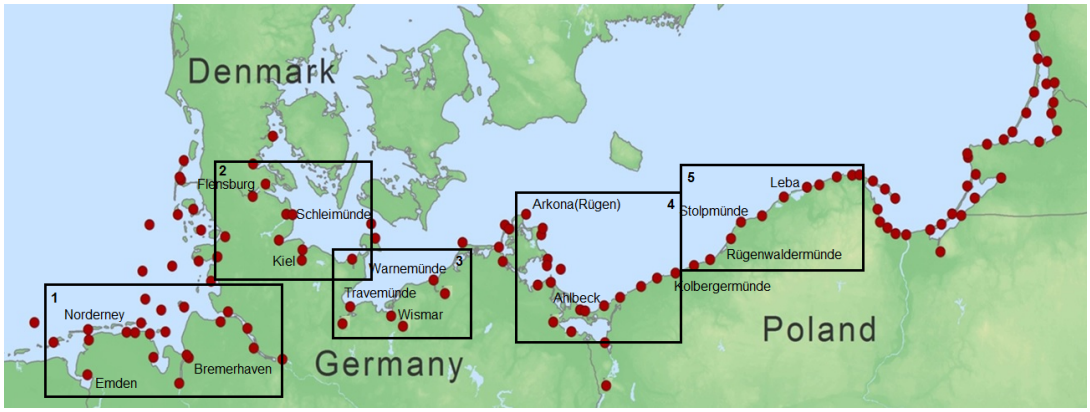

Figure 3.1.: Positions of 15 signal stations and their five boxes along the German Bight and the southern Baltic Sea coast.

A scatterplot of the yearly mean SLP data of each station in each box in Fig. 3.4 gives an idea of the spread of the data and serves as an assessment of the mean, the reference series, and how intense the mean is influenced by the data itself. For box 1, three values are out of the area of ± 5 hPa of the bisecting line. These data belong to the Emden-Norderney and Emden-Bremerhaven scatterplot. The scatterplot of Bremerhaven-Norderney is inbetween the ± 5 hPa area.

This implies that the data of the Emden time series influences the spatial mean series. At box 2, data of all station combinations are outside the ± 5 hPa area, which means, that for different time sections the mean is influenced by different station data. For box 3 the data belonging to Travemünde are outside the ± 5 hPa area. Therefore, the data of Travemünde has the highest influence. At box 4, it is Ahlbeck station and at box 5 it is Rügenwaldermünde, which influences the spatial mean of their boxes the most.

With the awareness that it is not possible to use a reference series, calculated from the candidate series, the SNHT is done to find shift non-homogeneity at this time series. The SNHT is applied on the yearly mean of each of the 15 series. Firstly, the difference of the candidate value and the reference value is calculated and named q. With the equations of 3.1 and the cumulutive sums the test value T is calculated. The test value T gives the opportunitiy of a non-homogeneity. Where the maximum of T occurs and is higher than a critical value, the probability of a non-homogeneity, starting in this year, is given. The critical value depends on the total number of data n and for the 95 % level 7.747 for n= 30 (Alexandersson and Moberg, 1997). That means,

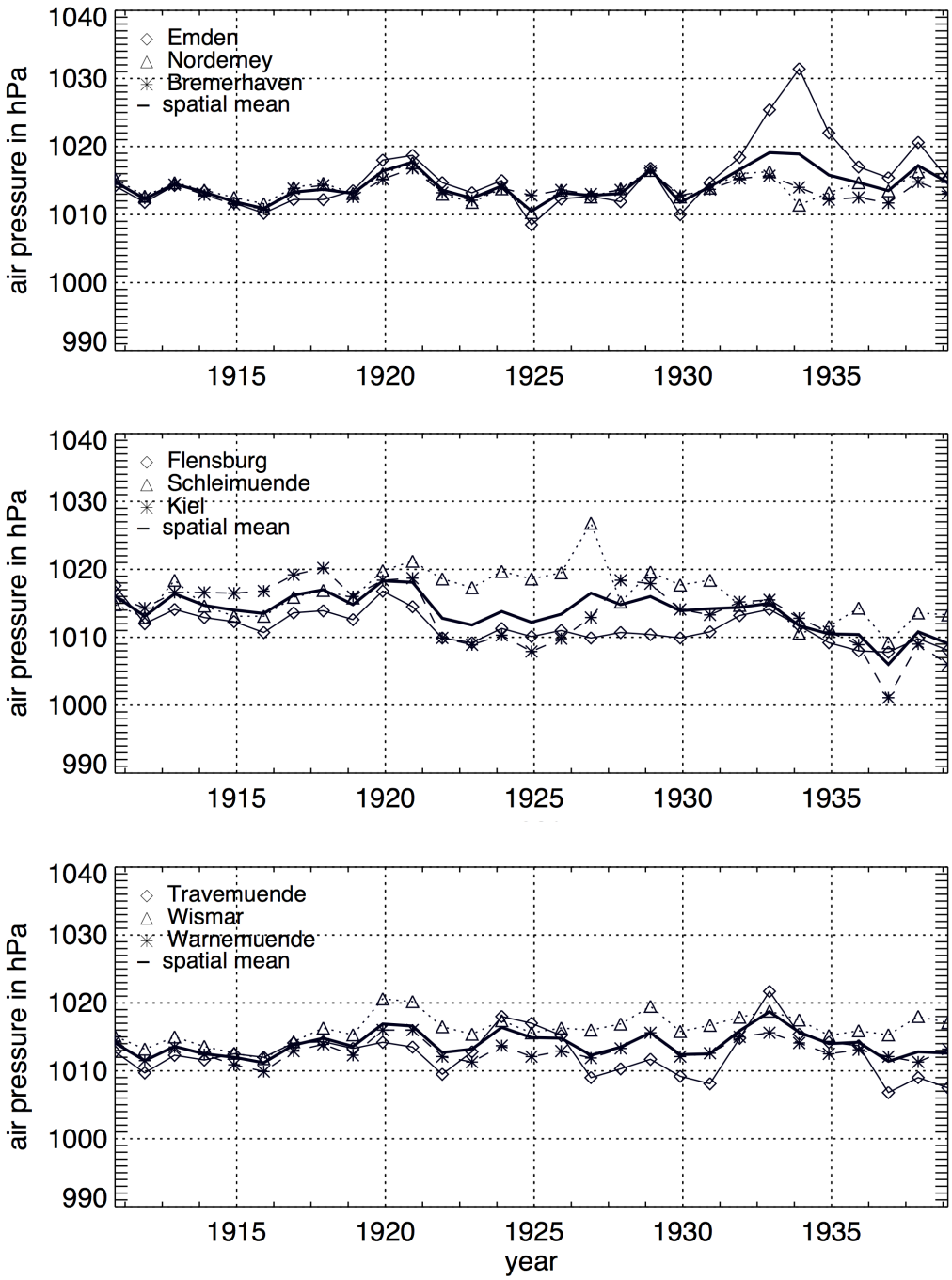

Figure 3.2.: Time series from 1910 to 1939 of SLP data and their spatial mean (solid line) of boxes 1 to 3 from the top to the bottom.

that with a probability of 95 %, a shift-non-homogeneity is given at this point. The calculated distributions of the test values T and the absolute differences q of all series are displayed in Figs. 3.5 to Figs. 3.8. The solid lines describe the difference q between the candidate value and the reference value, the as-

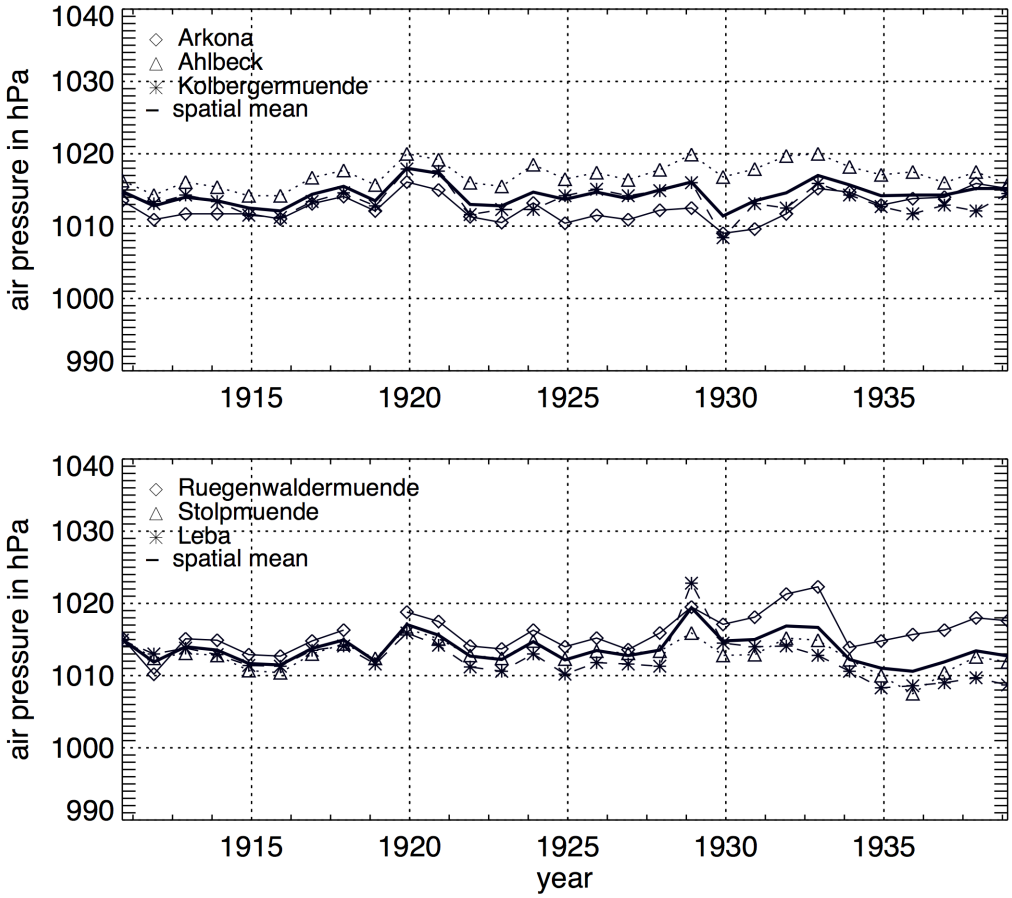

Figure 3.3.: Time series from 1910 to 1939 of SLP data and their spatial mean (solid line) of boxes 4 (top) and 5 (bottom).

terisks describe the test value T and the red vertical lines show the maximum of the test value T and the year of the beginning of a shift-non-homogeneity. The horizontal dotted line shows the critical value of the SNHT with 7.747 (Khaliq and Quarda, 2007).

In Fig. 3.5 the maximum of the test value T describes a shift-non-homogeneity in 1933 for Emden. For the series of Bremerhaven, a beginning of a non-homogeneity is detected in 1932. For both stations, q shows higher values after the detected year. Also, the test value series of Norderney shows at a maximum in 1932, but it is not higher than the critical value and a detection of a non-homogeneity is not given. Also for the Flensburg series a maximum of the test value is given in 1932, but does not reach the critical value. In Fig. 3.6 a non-homogeneity is found for Schleimünde station, starting in 1920. Wismar station and Travemünde station show multiple maxima of the test value. While at the series of Wismar station two further maxima are lower than the critical value, Travemünde shows two maxima higher than the critical value.

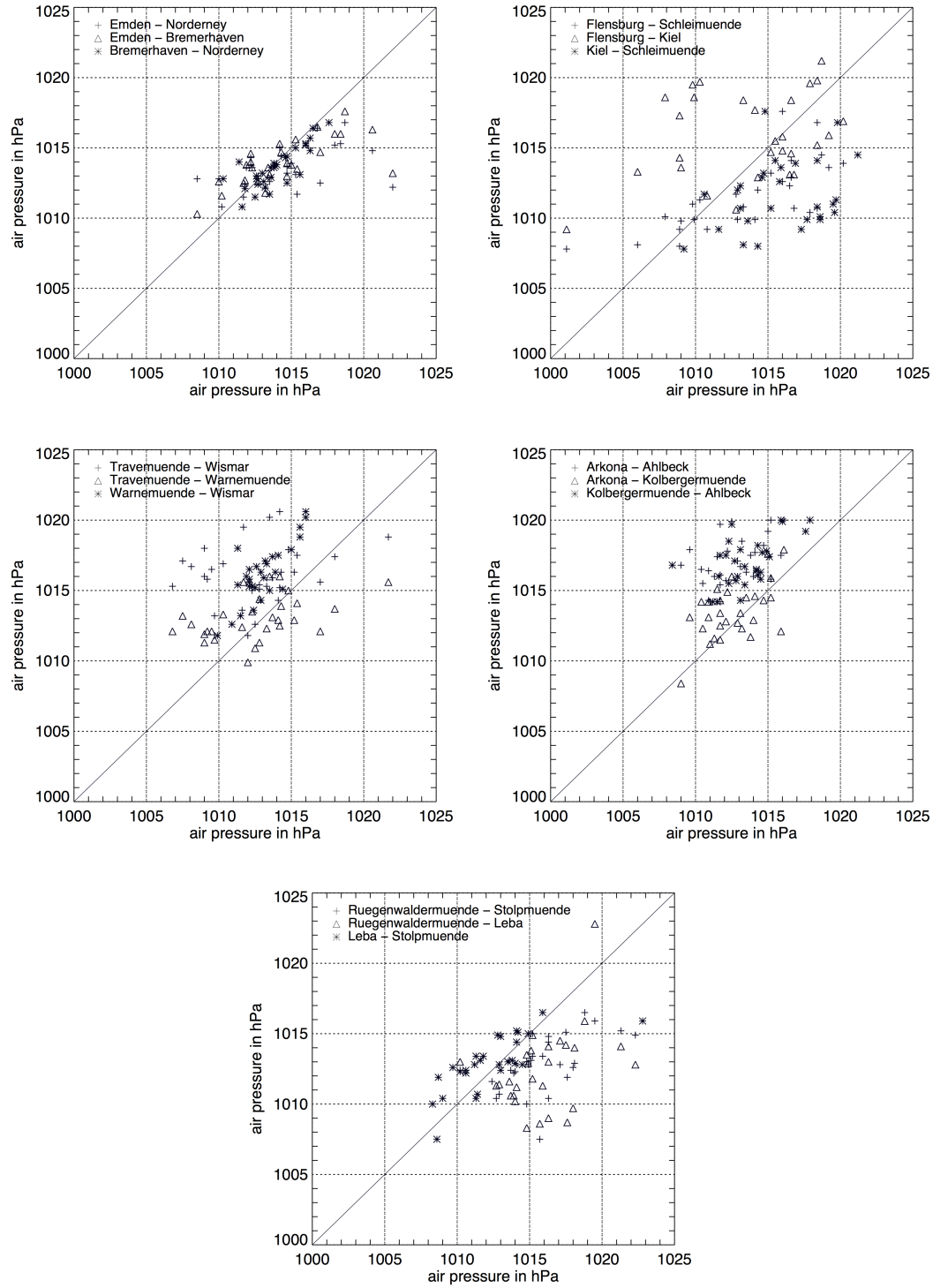

Figure 3.4.: Scatterplots of SLP data for each spatial box with three stations. From the top to the bottom and from left to right, it goes box 1 to box 5. The scatterplots show the spread of each SLP data and each station.

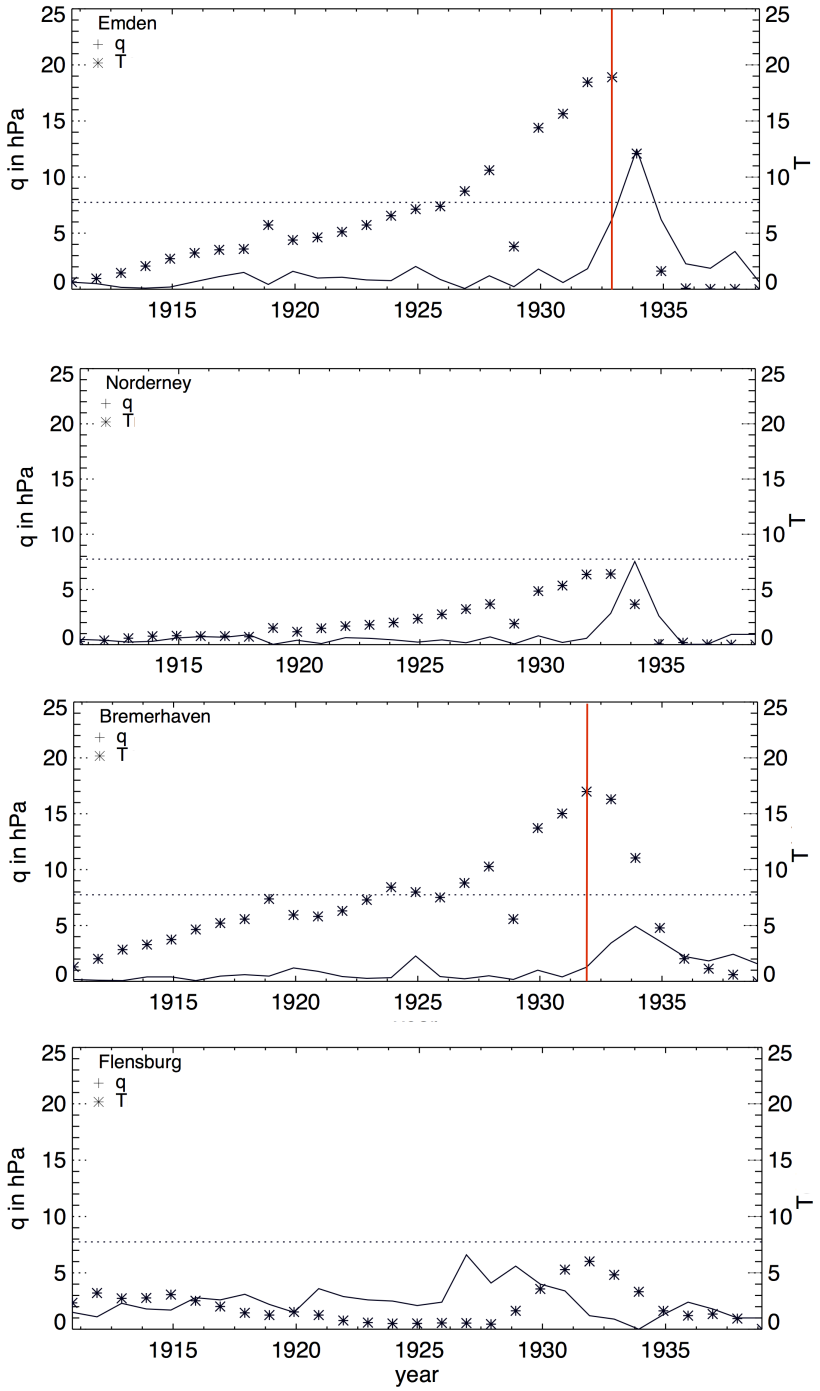

Figure 3.5.: Distribution of T-value and difference q of Emden, Norderney, Bremerhaven and Flensburg from the top to the bottom. The solid lines describe the difference q between the candidate value and the reference value, the asterisks describe the test value T and the red vertical lines show the maximum of the test value T and the year of the beginning of a shift-non-homogeneity. The horizontal dotted line shows the critical value of the SNHT with 7.747.

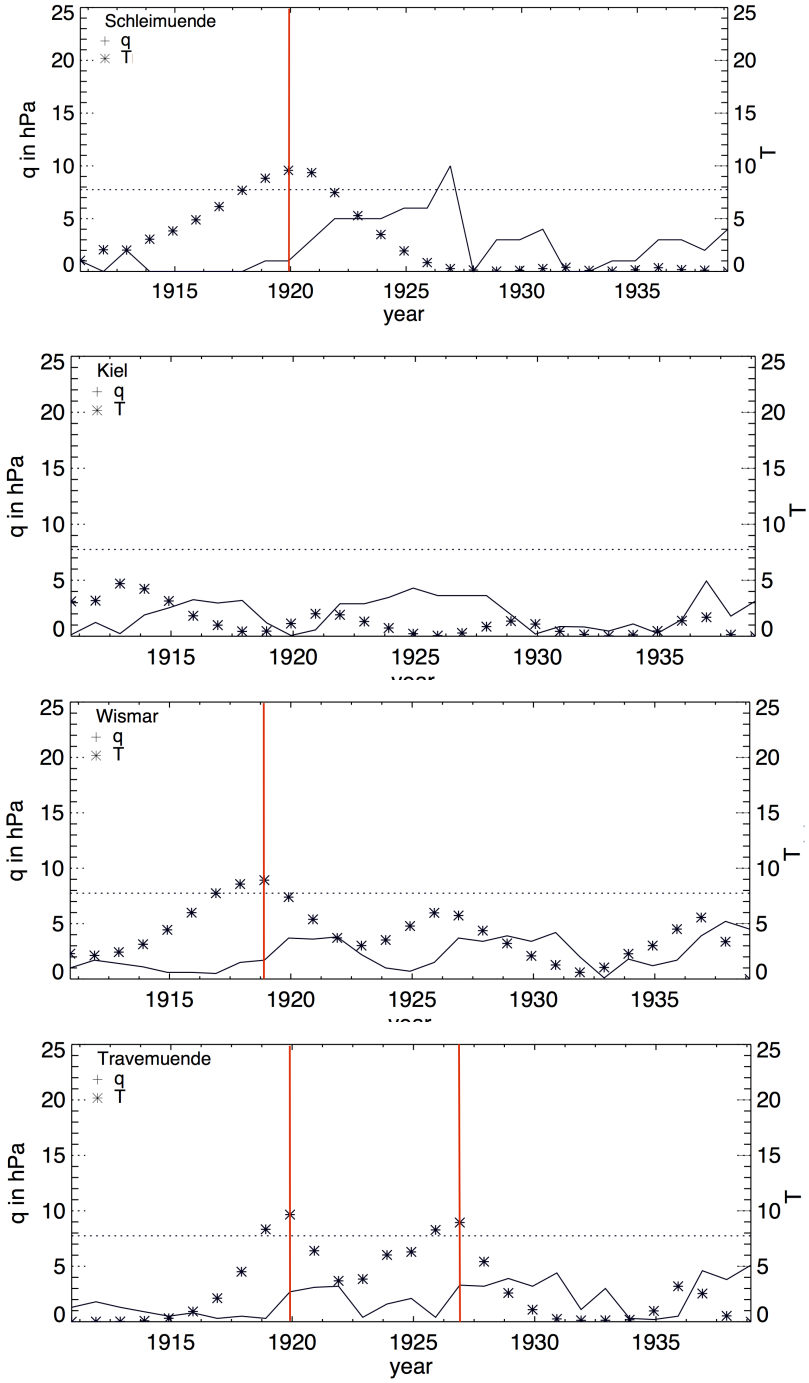

Figure 3.6.: Distribution of T-value and difference q of Schleimünde, Kiel, Wismar and Travemünde from the top to the bottom. The solid lines describe the difference q between the candidate value and the reference value, the asterisks describe the test value T and the red vertical lines show the maximum of the test value T and the year of the beginning of a shift-non-homogeneity. The horizontal dotted line shows the critical value of the SNHT with 7.747.

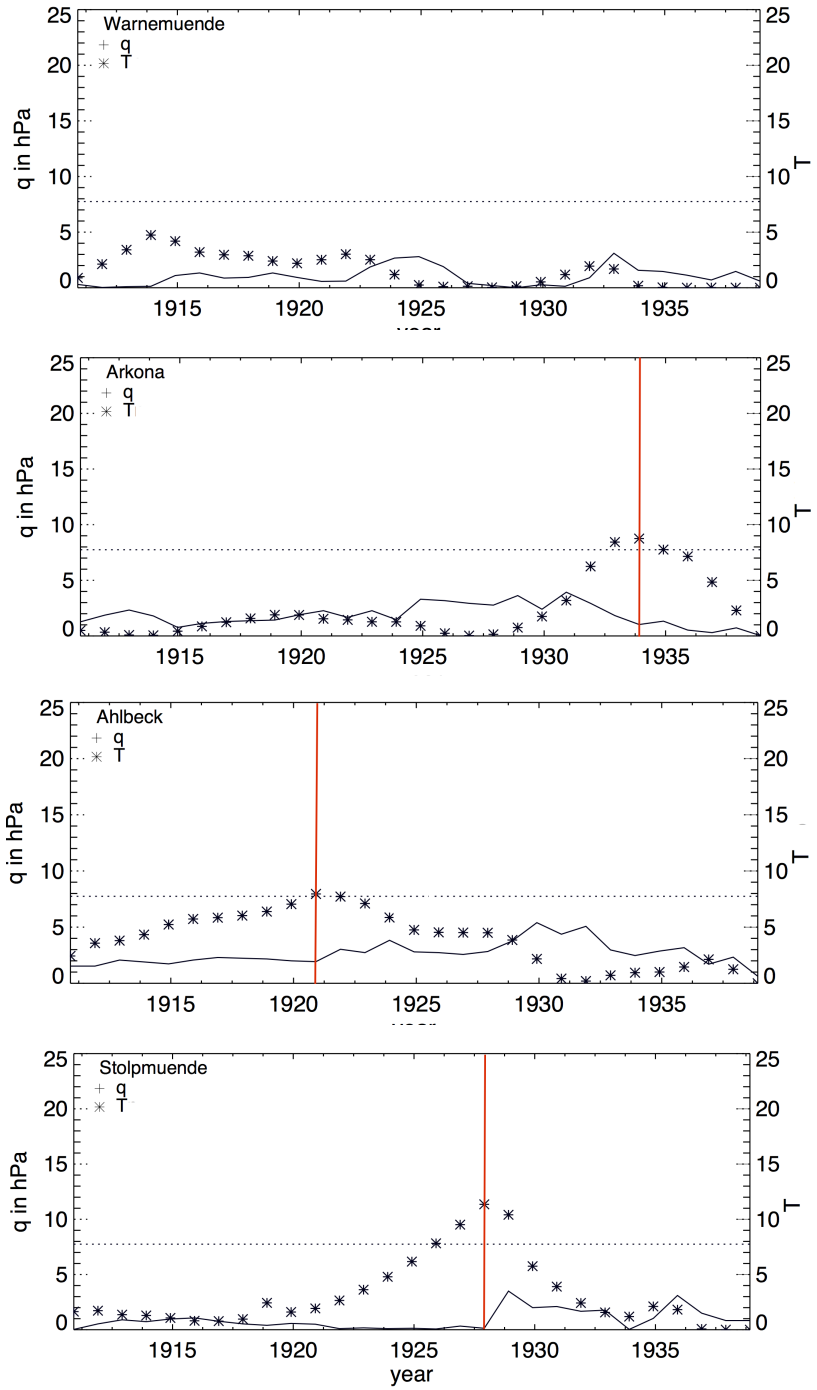

Figure 3.7.: Distribution of T-value and difference q of Warnemünde, Arkona, Ahlbeck and Stolpmünde from the top to the bottom. The solid lines describe the difference q between the candidate value and the reference value, the asterisks describe the test value T and the red vertical lines show the maximum of the test value T and the year of the beginning of a shift-non-homogeneity. The horizontal dotted line shows the critical value of the SNHT with 7.747.

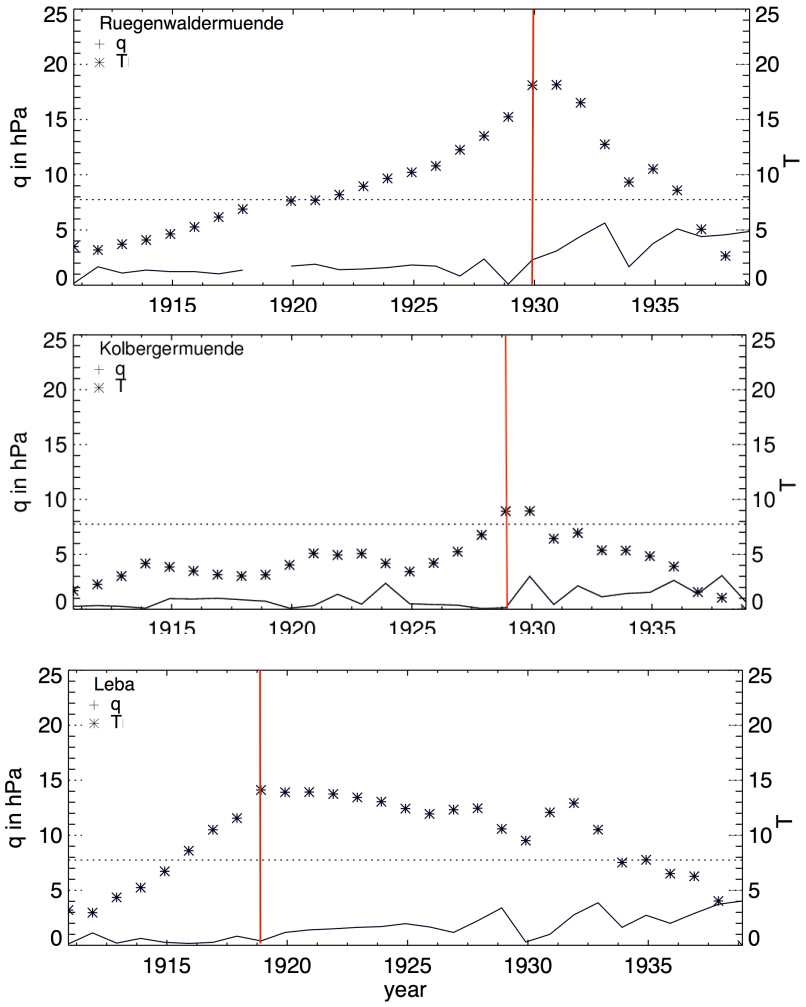

Figure 3.8.: Distribution of T-value and difference q of Rügenwaldermünde, Kolbergermünde and Leba from the top to the bottom. The solid lines describe the difference q between the candidate value and the reference value, the asterisks describe the test value T and the red vertical lines show the maximum of the test value T and the year of the beginning of a shift-non-homogeneity. The horizontal dotted line shows the critical value of the SNHT with 7.747.

For Kiel station no shift-non-homogeneity is detected with a probability of 95 %. For Arkona, Ahlbeck and Stolpmünde station, non-homogeneity can be detected in 1934, 1921 and 1928 (Fig. 3.7). The test value T for Warnemünde station shows no non-homogeneity during these time period from 1910 to 1939. For the three stations of box 5, Rügenwaldermünde, Kolbergermünde and Leba (Fig. 3.8), a non-homogeneity can be detected with the SNHT for each station, as described before. For Rügenwaldermünde the beginning of the non-homogeneity is detected in 1930, for Kolbergermünde in 1924 and

Table 3.1.: List of stations with the year of the beginning of the non homogeneity and the T-value.

Station	Year of non-homogen.	T
Emden	1932	19
Bremerhaven	1932	17
Schleimünde	1920	10
Wismar	1919	9
Travemünde	1920/1926	10/9
Arkona	1934	8
Ahlbeck	1921	7
Stolpmünde	1928	12
Rügenwaldermünde	1930	18
Kolbergermünde	1929	9
Leba	1919	14

for Leba in 1919. All in all, there are eleven of 15 stations with a detected non-homogeneity and the results are summarized in table 3.1.

Homogenization of SLP Data The next step to detect a non-homogeneity is the homogenization of the time series. The method of Easterling and Peterson (1992) is used for the homogenization of the given SLP time series and is described hereinafter. The mean of q is calculated for the data before the estimated starting point of an inhomogeneity and after this point. The difference of these two averages is added or subtracted with the candidate series values, which depends on a lower or higher partly mean of the candidate value. This is done for the eleven time series, where a non-homogeneity is detected. Figs. 3.9 to 3.11 show the homogenized time series.
The homogenized SLP time series of Emden, Bremerhaven, Schleimünde and Wismar station are shown in Fig. 3.9. The red line is the new calculated time series for each station and the black line the original time series. For Emden station the huge peak between 1931 and 1936 is eliminated by the method described before. The original values between 1931 and 1936 are subtracted by 4.36 hPa, which is the difference of the mean of q before and after 1931 ($\bar{q}_{before} - \bar{q}_{after}$), where a beginning of a non-homogeneity is detected. For Bremerhaven station the original series is adjusted, between 1931 and 1935, by -2.5 hPa in this period. The data of Schleimünde station are homgenized for a time period of 14 years between 1918 and 1931. The original series is decreased by 3.0 hPa during these 14 years. The peak between 1925 and 1927, is too short, only three years, to be eliminated by this method of yearly means.

The time series of SLP data of Wismar station, also in Fig. 3.9, is homogenized by subtracting 1.7 hPa of the original value during the time period of 1919 and 1939. The length of the homogenized time period depends on the algebraic sign of z_i (3.1). For a negative z_i time period, longer than five years, the difference of the means is added and for a positive z_i, the difference of the means is subtracted. Fig. 3.10 shows the homogenized series of Travemünde, Arkona, Ahlbeck and Kolbergermünde station. For Travemünde station different time periods are separated. This time series shows two maxima at the SNHT. Therefore, a subtraction of 1.5 hPa at the time period of 1924 to 1926 is done followed by an addition of 2.2 hPa for 1927 to 1931 and a subtraction of 2.2 hPa between 1931 and 1935. For Arkona station a subtraction of 1.26 hPa, between 1933 and 1939, is done. For the time series of Ahlbeck station two subtractions of 1.06 hPa are done between 1922 and 1926 and between 1927 and 1933. At Kolbergermünde, the original time series is decreased, between 1932 and 1938 by 1.16 hPa. Fig. 3.11 shows the homogenized time series of Rügenwaldermünde, Stolpmünde and Leba station.

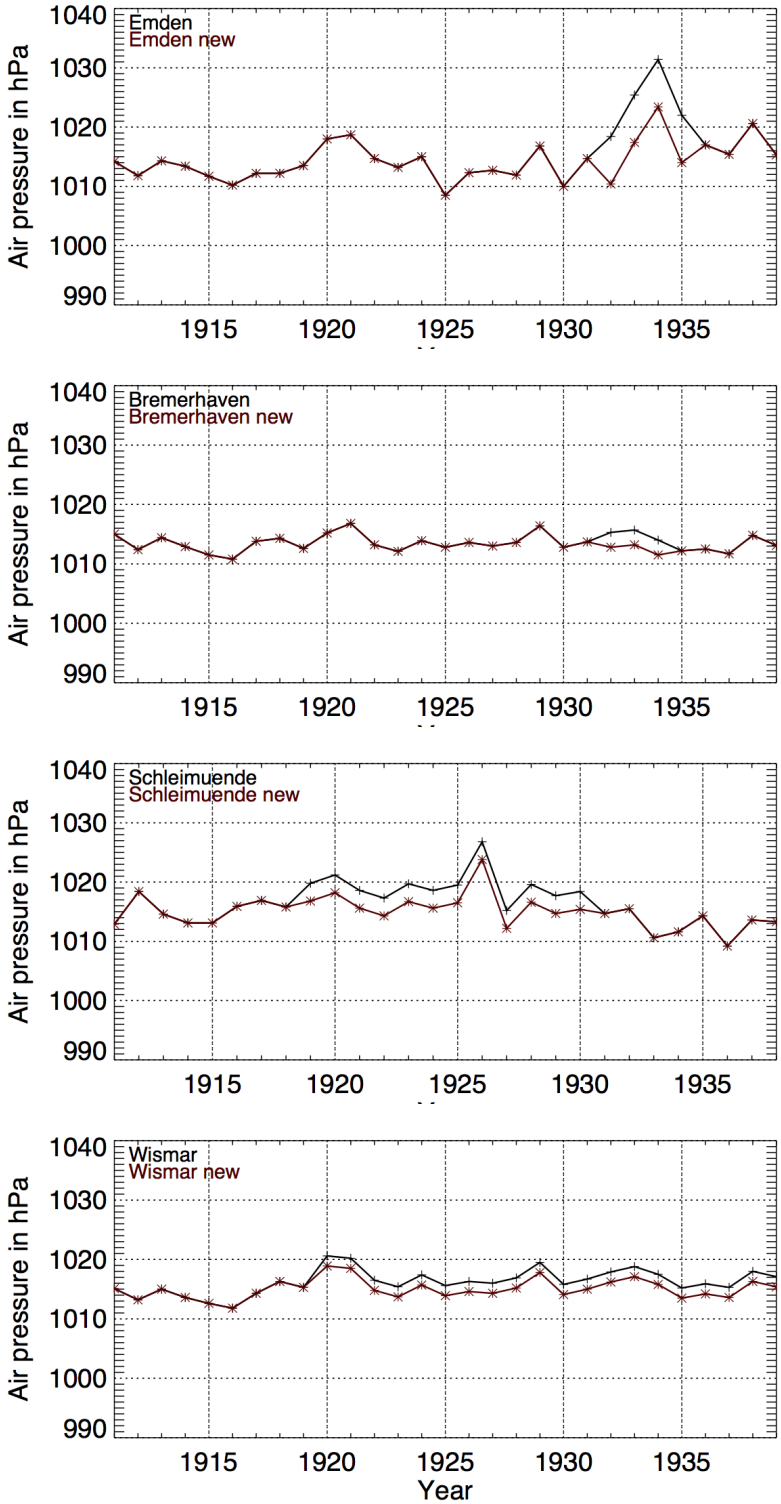

Figure 3.9.: Homogenized time series of SLP data for Emden, Bremerhaven, Schleimünde and Wismar. The red line describes the homogenized time series and the black line the candidate series.

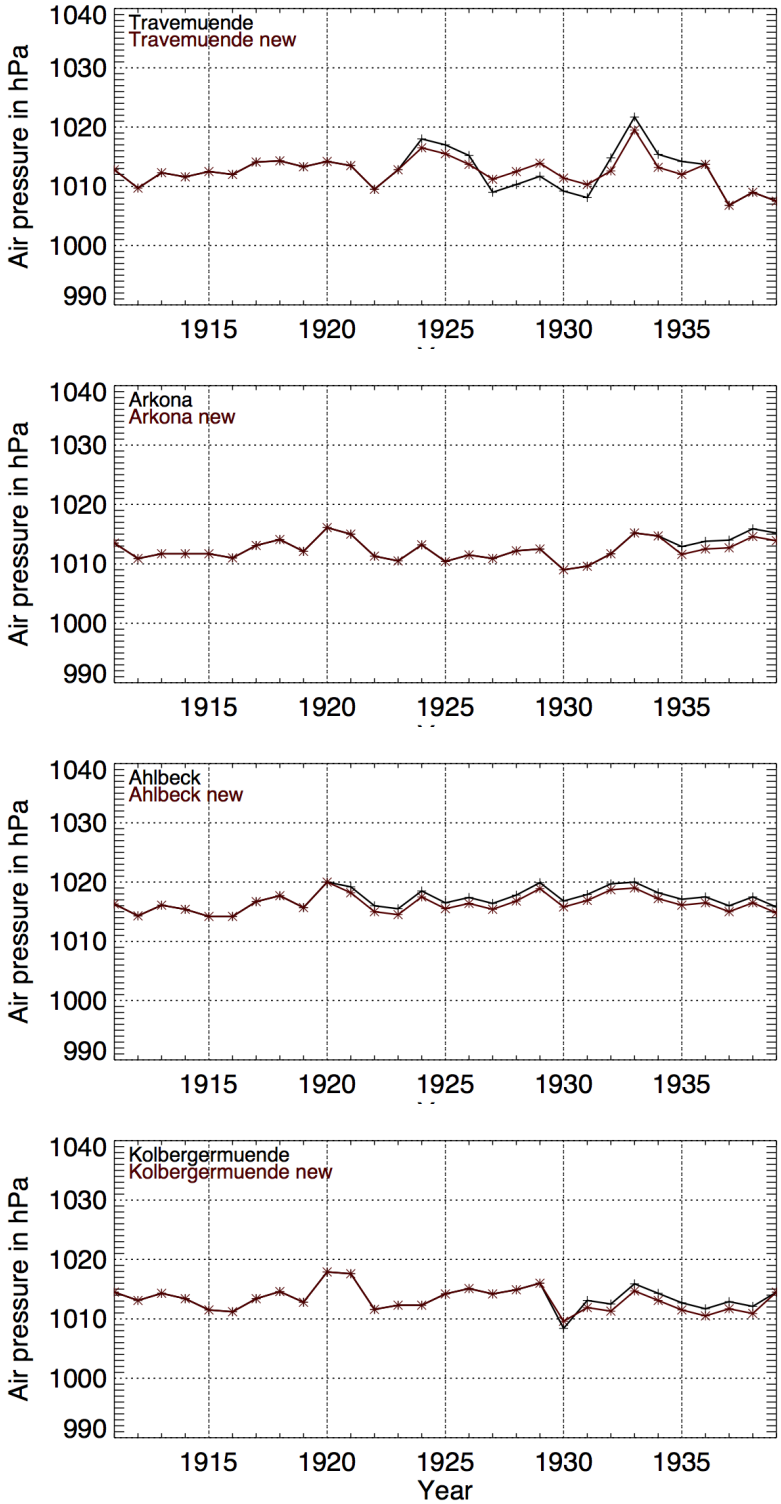

Figure 3.10.: Homogenized time series of SLP data for Travemünde, Arkona and Ahlbeck. The red line describes the homogenized time series and the black line the candidate series.

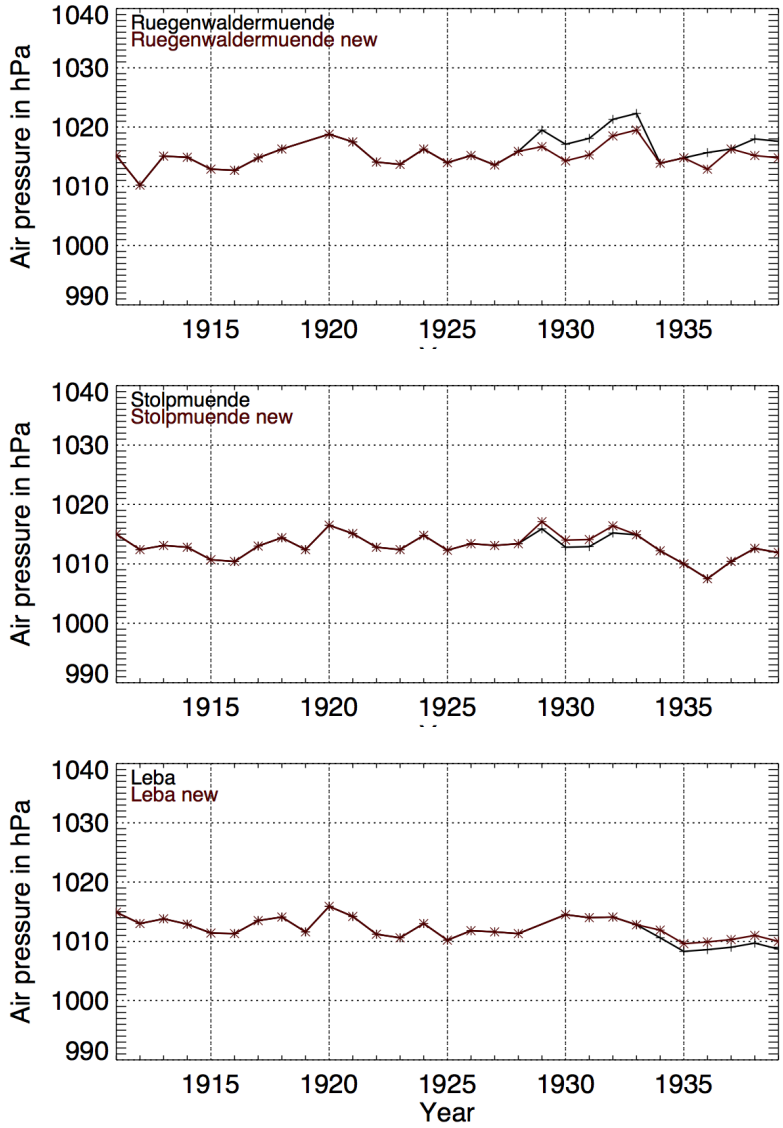

Figure 3.11.: Homogenized time series of SLP data for Rügenwaldermünde, Stolpmünde and Leba. The red line describes the homogenized time series and the black line the candidate series.

For Rügenwaldermünde the homogenization starts in 1930 and ends in 1939 with an interruption in 1935. The value of 3.01 hPa is subtracted from the origional value. The time series of Stolpmünde shows an addition of 1.24 hPa between 1928 and 1932. For Leba station in Fig. 3.11, the algebraic sign of z_i changes nearly every year from the begining of the detected non-homogeneity in 1919 until 1931. Therefore, the homogenization process starts in 1931 with an addition of 1.73 hPa of the origional time series until 1939. The table 3.2 summarizes the results.

Table 3.2.: List of stations with the difference of the means of q before and after the inhomogeneity in hPa and the time where the difference is applied.

Station	$\bar{q}_{before} - \bar{q}_{after}$ in hPa	time period for homogen.
Emden	-4.36	1931-1936
Bremerhaven	-2.50	1931-1935
Schleimünde	-3.0	1918-1931
Wismar	-1.70	1919-1931
Travemünde	-1.50	1924-1926
	+2.20	1927-1931
	-2.20	1931-1935
Arkona	-1.26	1933-1939
Ahlbeck	-1.06	1922-1936
	-1.06	1927-1933
Stolpmünde	+1.24	1928-1932
Rügenwaldermünde	-3.01	1928-1933
	-3.01	1934-1939
Kolbergermünde	+1.16	1932-1938
Leba	+1.73	1931-1939

3.3 Conclusion

The homogenization of observation data is necessary to try to recognize trends in a time series. For the 15 signal stations, it is possible to find inhomogeneities by the SNHT, which is a well tested homogeneity test. It can be remarked that not all 15 time series of yearly means show an inhomogeneity and the detected inhomogeneity is acceptable for further investigations in the yearly means. To find further shifts during this time period an estimation of monthly means should be used or the time series has to be longer. During a time period of 30 years it is difficult to find an inhomogeneity smaller than three years, because the probability to find a real non-homogeneity is decreased the shorter the estimated period is.
The reasons why a non-homogeneity could appear during observation, is that mistakes can go along with the recalculation from mmHg to hPa and it is possible that not all SLP data were reduced to **NAN!** (**NAN!**) during observation. The homogenization of the signal station data could be improved by having more information about the single signal stations, but information about dislocation of stations or something else are not documented. However, the SLP

data of signal stations, observed during the time period from 1910 to 1939, can be homogenized in their yearly means and can be used for further scientific investigations.

4 Evaluation of Storminess by Wind and Air Pressure Data

The expansion of knowledge of past, current and future changes of the storminess in Northern Europe plays an important role to predicting possible storm surges along the coasts of the German Bight and the southern Baltic Sea. The disclosure of trends in storminess from wind observations is almost impossible because of insufficient homogeneity and the lack of long-term records in the wind data series. Furthermore, ship observations are available since the 19th century, but vary in time and space. Therefore, calculations of the geostrophic wind have to be proved as a valuable proxy for wind
(Krüger and von Storch, 2011). The geostrophic wind depends on air pressure. The air pressure is a parameter, other than wind, whose measurement is not influenced by a changing landscape over the time and is almost independent from the observing altitude. Hence, the geostrophic wind can be calculated by triangles, which are spanned by three stations
(Schmidt and von Storch, 1993). These triangles could also be spanned over water areas, where only rarely wind observation data are only rarely available. The finding of three stations with observation data for the same length of time series is often quite difficult.
The SLP data of signal stations could be valuable for a regional calculation of the geostrophic wind at the German coasts, but are only available until 1939. In order to use the oppertunity to also use reanalysis data for estimation, the calculation of the geostrophic wind at the German Bight and the southern Baltic Sea is done by SYNOP-data as available observation data from 1967 to 2012. The results of the calculation of the geostrophic wind from SYNOP-data and the comparison with reanalysis data should give the possibility to extend the time series by signal station data for the German coastal regions and get an estimation of long-term trends of storminess in the German coastal regions, and the German Baltic Sea coast.

Current and past studies on long-term trends of storminess do not show a significant decrease or increase of storminess in North Europe. Feser et al. (2015) gives an overview of 122 studies depending on trend analysis of storminess in Northern Europe for proxy and observation data as well as for reanalysis

and model data for the past. For the North Sea area, six studies on proxy and observation data render no significant trend during the last 100 years (Schmidt and von Storch (1993), Alexandersson et al. (2000) and Wang et al. (2009)). Three out of ten studies of observation data for the North Sea region indicate a decrease in storminess in the last 100 years (Cusack (2013) and Ciavola et al. (2011)) and one study an increase (Carter and Draper, 1988).
For the Baltic Sea area 24 studies about trend analysis in storminess exist. Out of the 24 studies, 17 time series of them are longer than 100 years.
Bärring and von Storch (2004) and Bärring and Fortuniak (2009) show, especially for Sweden, no long-term trends in storminess. Also the WASA (1998) study rendered no trend in storminess back to about 1880. Out of the 24 studies, eight studies provide a decrease in storminess in the Baltic Sea area. Especially studies of the geostrophic wind from triangles in Sweden and Finland (Suvilampi (2009) and Wern and Bärring (2009)) show a decrease in storminess. For coastal areas in Sweden the wind trend study of Minola et al. (2016) show also decreasing trends for coastal areas.
The results of reanalysis and model data studies for past decades show for the North Sea area more decreasing storminess trends than no trends. Increasing trends could not be found in these studies. Brönnimann et al. (2012) and Donat et al. (2010), as well as Weisse et al. (2005) denote a decreasing of storminess by reanalysis data, where Brönnimann et al. (2012) and Donat et al. (2010) examine time series of more than 100 years for the North Sea area. The study of Smits et al. (2005) for the Netherlands by the NCEP/NCAR reanalyses and the ECMWF shows an increasing trend.
For the Baltic Sea, more decreasing trend results could be found than no trends by reanalysis and model studies for the past decades, for example, (Wang et al., 2011). The study by Hofherr and Kunz (2010) about the extreme wind climatology in Germany in the years between 1971 and 2000, examined by the ERA-40 reanalyses, does not show any trend for the German Baltic Sea coast. However, there are a lot of studies about storm trend analysis for the last 100 to 150 years by proxy, observation, reanalysis and model data. There are large decadal variations and no significant trend results, decreasing, increasing or constant, in storm numbers for the North Sea or Baltic Sea regions.

The longest time series of wind data over 120 years exists from the signal station Travemünde, which is located at the German Baltic Sea coast. The

wind direction and wind force data are analyzed in section 4.3 in regard to the North Atlantic Oscillation (NAO)-Index.
Firstly, an introduction to the used data and the triangle method is given in the following section. In a second part, the calculated time series of the percentiles of the geostrophic wind, derived from observation data, are compared with the reanalysis data. For the period from 1960 to 2012, time series of percentiles of the geostrophic wind are derived from synoptic SLP data for the German Bight and the southern Baltic Sea area. The results are compared to the same calculations for the coastDat2 dataset and the NCEP/NCAR reanalyses. The third part includes the analysis of long-term wind observations from signal stations.

4.1 Data

For the following evaluation, several different data types are used. Firstly, observational data of the routine network of the DWD and for the Hammer Odde (Bornholm) station from the Danish Meteorological Institute (DMI) are analyzed and compared with reanalysis data of the coastDat2 dataset, developed at the HZG, and the NCEP/NCAR reanalysis data. For further investigations the calculation process of the geostrophic wind from SLP data is necessary and described in the fourth part of this section. The wind data from signal stations are examined in section 4.3. A detailed description of signal station data and their quality is given in chapters 2 and 3.

4.1.1 Observational Data

For the calculation of the geostrophic wind SLP and air temperature data are required. Therefore, the observational SLP and air temperature data, called SYNOP-data, from the DWD-database and the SLP data of the historical climate data collection of the DMI are used. The DWD-database includes hourly meteorological observational data from all over Europe. In addition to the data of German stations, data from the Copenhagen station in Denmark are also used. The observational data of the DWD-database starts in 1960 and ends up till now. The historical climate data collection of the DMI includes observation data of seven Danish stations with data from 1868 to 2012.

The air pressure data from 1872 to 2012 are provided for the analysis of the geostrophic wind over the southern Baltic Sea. An overview of all existing historical climate data in Denmark is given in Cappelen (2013).
In table 4.1 the stations, which are used in the following calculation of the geostrophic wind over the German Bight and the southern Baltic Sea are listed with the station name, the latitude and the longitude, the elevation height, the used time period, the frequency of observations with the observation hours and the owned institutes. For all stations, except Hammer Odde, also air temperature data exist, which are used for the calculation of the air density, which is needed for the calculation of the geostrophic wind. For the calculation of the geostrophic wind of Hammer Odde station, where the air temperature data are not available, the air density of the standard atmosphere of 288.15 K is assumed.

Table 4.1.: List of stations used for the evaluation of the geostrophic wind, with the station name, the latitude and longitude, the elevation in m, the time period with available SLP and air temperature data (except Hammer Odde), the frequency of observations with the observation hours and the owned institutes.

Name	Lat. Lon.	Elev. in m	time period	obs. period	obs. h. (UTC)	Institutes
Copenhagen (DK)	N55.68/ E12.58	24	1965-2012	1966-1977 1977-2005 2005-2012	0,6,12,18 0-21 every 3h 0-23 every h	DWD
Emden (GER)	N33.70/ E7.15	1	1965-2012	1967-1977 1977-1981 1981-2012	6,12,18 6-18 every 3h 0-23 every h	DWD
Hamburg (GER)	N53.55/ E10.0	6	1965-2012	1967-1977 1977-1981 1981-2012	0,6,12,18 0-21 every 3h 0-23 every h	DWD
Hammer Odde (DK)	N55.30/ E14.77	7	1878-2012	1874-1987 1987-2001 2001-2012	7,13,20 3-21 every 3h 0-23 every h	DMI
List/Sylt (GER)	N54.92/ E8.33	2	1965-2012	1967-1977 1977-1981 1981-2012	6,12,18 0-21 every 3h 0-23 every h	DWD
Rostock (GER)	N54.08/ E12.13	3	1965-2012	1966-1977 1977-2012	0,6,12,18 0-23 every h	DWD
Schleswig (GER)	N55.16/ E9.25	1	1965-2012	1966-1977 1977-1981 1981-2012	0,6,12,18 0-21 every 3 h 0-23 every h	DWD

4.1.2 Reanalysis Data

Observational wind data are often inhomogeneous and have an insufficient quality due to observational errors, for this reason model or reanalysis data are used for calculations or analyses of atmospheric questions. An overview of common reanalyses is given in chapter 1. For the following analysis of the geostrophic wind, two different reanalyses are used to estimate the observational data. Firstly, an introduction to the coastDat reanalyses is given, followed by an introduction to the NCEP/NCAR reanalyses.

NCEP/NCAR
The NCEP/NCAR reanalyses uses analyses and forecast systems to perform data assimilations by using past data. The data are provided in 4-times daily, daily and monthly values for 1948 to the present. Long-term monthly means are derived from data for the time period from 1981 to 2010. The global grid of the reanalysis data consists of 17 pressure and 28 sigma levels. The data are available in a resolution of $2.5\,^{\circ} \times 2.5\,^{\circ}$. The values of air temperature, potential temperature, relative humidity, SLP, u-wind and v-wind, the geopotential height and a land-sea mask are available. For the following calculation daily SLP and air temperature data from 1960 to 2012 are used.

CoastDat
The coastDat reanalyses, developed at the HZG, are high resolution regional atmosphere reanalyses to assess long-term changes, variability and the trends of atmospheric and oceanic conditions in coastal regions. The acronym coastDat stands for set of consistent ocean and atmospheric data. As stated in (HZG, 2016), coastDat was integrated to improve the observational database and increase data homogeneity and consistency.
For coastDat reanalyses two dataset, 1 and 2, were generated. CoastDat1 provides atmospheric and oceanic data over Europe and the North Atlantic with a resolution of $0.5\,^{\circ} \times 0.5\,^{\circ}$ and an hourly output of SLP, wind speed and direction and 2 m air temperature data for the atmosphere from 1948 to 2007. Oceanic data are available for the North Sea region, which provide hindcast and scenario data. For the atmospheric data in coastDat, NCEP/NCAR reanalyses were used as forcing data in combination with spectral nudging (Weisse et al. (2009) and Geyer (2014)).

Table 4.2.: CoastDat2 and NCEP/NCAR reanalyses overview of the used atmosphere SLP and air pressure data with the available time period, the resolution, the coverage and the institute.

	Time period	Resolution	Coverage	Institute
CoastDat2	1948-present	0.22° × 0.22°	Regional	HZG
NCEP/NCAR	1948-present	2.5° × 2.5°	Global	NCEP/NCAR

Similar to the coastDat1 dataset, the coastDat2 contains atmospheric data for Europe and the North Atlantic Ocean, but in addition it also includes atmospheric data for parts of Asia and the diversion part of the Pacific Ocean. The oceanic data are generated with a finer resolution up to 1.6 km×1.6 km over the North Sea and the Baltic Sea area. For the atmosphere a resolution of 0.22 °× 0.22 ° with an hourly output of SLP, wind speed and direction, air and dew point temperature in 2 m, cloud cover and heat fluxes is available. The hindcast data are available from 1948 to the present. Also, scenario data are available from 1948 to 2100 with a resolution of 0.2 °× 0.2 ° and an hourly to 3-hourly output.
An overview of the NCEP/NCAR and coastDat2 data is listed in table 4.2

4.2 The Geostrophic Wind at the German Coasts

The geostrophic wind is a good proxy for the free atmospheric wind speed (Krüger and von Storch, 2011). Time series of the geostrophic wind are calculated for observational and reanalysis data for three triangles at the German Bight and the southern Baltic Sea using the triangle method. This method was introduced by Schmidt and von Storch (1993) for the German Bight.
One of the three triangles is located in the German Bight and spans the area between Hamburg, Norderney and List. Two further triangles cover parts of the southern Baltic Sea region. One of them describes the area between Schleswig, Rostock and Copenhagen and the second one the area between Rostock, Copenhagen and Hammer Odde. Fig. 4.1 shows the positions of the three triangles, for which the geostrophic wind time series is calculated. The calculation of the geostrophic wind in the triangle area consists of solving a system of three linear equations (Schmith (1995) and Wang et al. (2009)). Furthermore, the median and the 95th percentile of the geostrophic wind speed are derived by monthly means. The 95th percentile indicates that 5 %

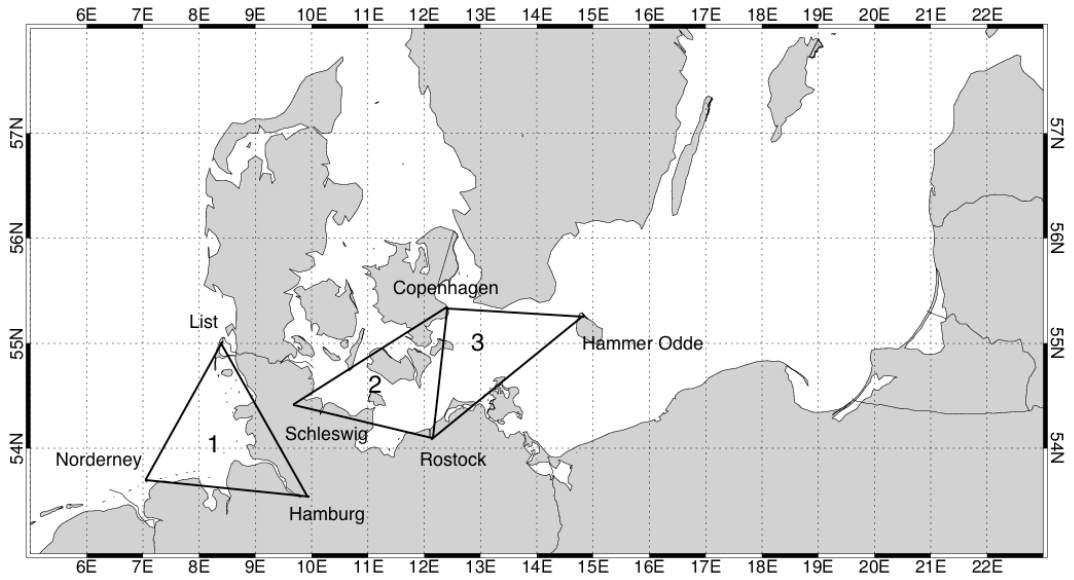

Figure 4.1.: Positions of triangles for the calculation of the geostrophic wind. One triangle is spanned over the German Bight with the stations Hamburg, Emden and List (triangle 1). A second triangle is spanned over the western Baltic Sea with the stations Rostock, Schleswig and Copenhagen (triangle 2). A third triangle is spanned over the southern Baltic Sea with the stations Copenhagen, Hammer Odde and Rostock (triangle 3).

of the data have higher values than the one in the 95th percentile and the median gives values for which 50 % are higher and 50 % are lower. Fig. 4.2 shows the time series of the 95th percentiles and the median of the calculated geostrophic wind for the three triangles. The different line colours indicate the different triangles. The median, solid lines, and the 95th percentiles and broken lines show variations of the geostrophic wind during the time period with no significant trend. A higher wind speed for the German Bight area in comparison with the Baltic Sea area is to be expected. The 95th percentiles of SYNOP-data show higher values in the time period between 1990 and 2004. Before 1990 and after 2004, the percentiles of the wind speed data are not clearly higher. The median wind speed data do not show higher wind speed values for the German Bight area over the whole time period from 1968 to 2012.

The calculation of the geostrophic wind from reanalyses data are done in a second step. For this, the coastDat2 dataset and the NCEP/NCAR reanalysis data are used. The station points are taken from the datasets, as the weighted mean of the four nearest grid points in each geographic direction. Time series

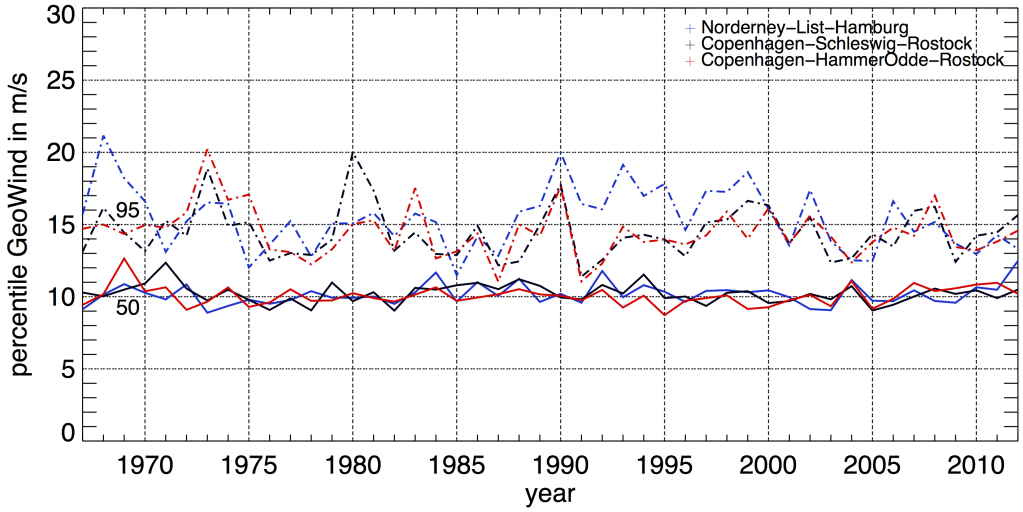

Figure 4.2.: Time series of the 95th percentile (dashed lines) and median (solid line), derived by monthly means, of the geostrophic wind for the three given triangles by SYNOP-data. The blue lines indicate triangle 1, the red lines triangle 2 and the black lines triangle 3.

of the percentiles of the geostrophic wind for coastDat2 and NCEP/NCAR data are shown in Fig. 4.3.

The geostrophic wind speed, calculated from the CoastDat2 dataset, varies slightly around 10 m/s for the median and 15 m/s for the 95th percentile for the triangles located over the Baltic Sea (triangle 2 and 3). For triangle 1, which is located over the German Bight, a higher level can be observed for the whole time period. The geostrophic wind speed of triangle 1 is about 6 m/s higher for the 95th percentile about 2 m/s higher for the median. For all three triangles light peaks can be detected in 1982 and 1990, but no significant trend of the geostrophic wind speed is visible. The calculated geostrophic wind speed from the CoastDat2 dataset agree with the calculated geostrophic wind speed from the observational data in Fig. 4.2.

The time series of the calculated geostrophic wind speed from the NCEP/NCAR data show strong variations for all three triangles in the median and the 95th percentiles. These higher variations, in comparison to the geostrophic wind speed time series calculated from observational and CoastDat2 data, are due to the lower resolution of the NCEP/NCAR data. The lower resolution of the NCEP/NCAR data are also caused by having nearly the same course of the two time series of the triangles located over the Baltic Sea. The nearly same course of triangle 2 and 3 is caused by the positions of the triangles in

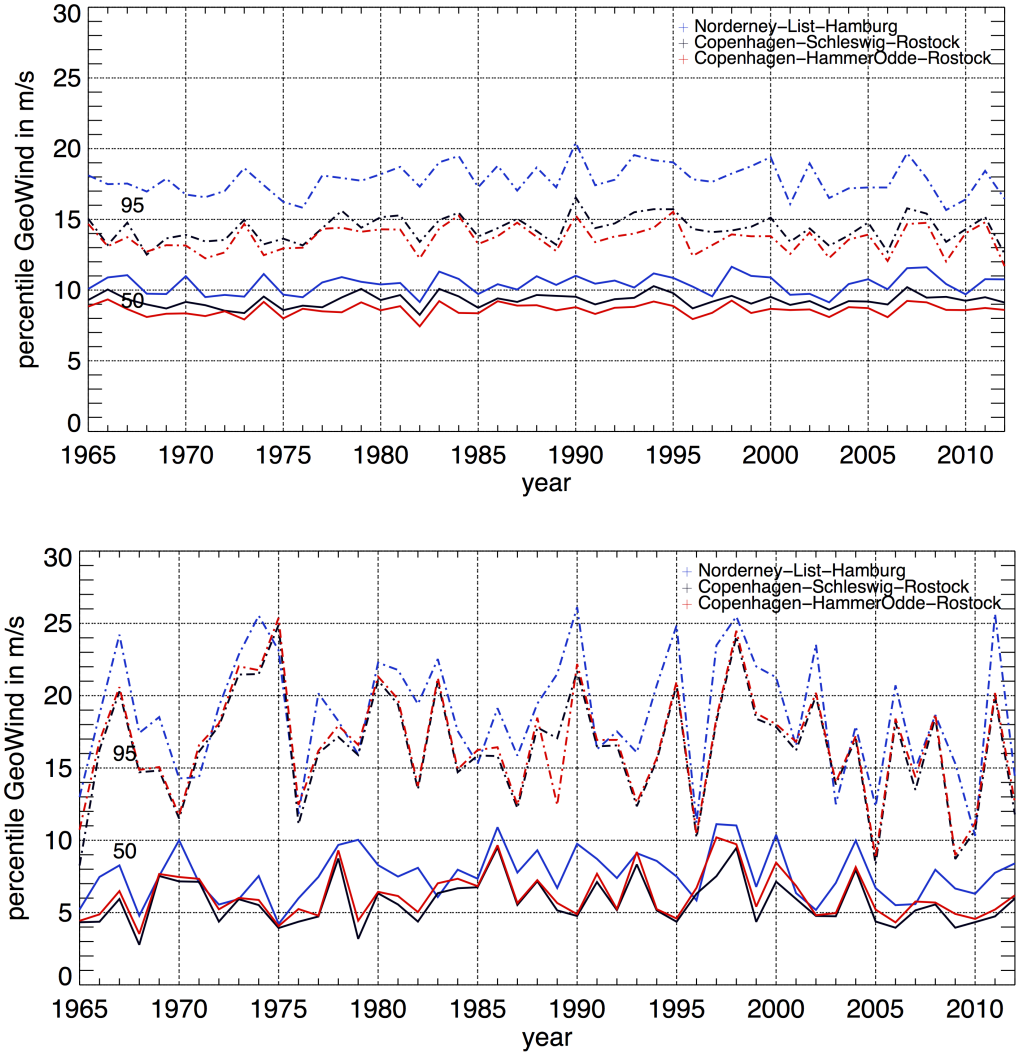

Figure 4.3.: Time series of the 95th percentile and the median of the geostrophic wind of the three given triangles. The blue lines indicate triangle 1, the red lines triangle 2 and the blue lines triangle 3. The time series of the 95th percentile and the median of the geostrophic wind of coastDat2 data are shown in the top and the geostrophic wind speeds of the NCEP/NCAR data in the bottom.

the same grid box caused by a lower resolution of the NCEP/NCAR data. A further distinctive feature in comparison to the observational and coastDat2 data is the lower level of about 3 m/s for the median in all three triangles. Also higher wind speeds for the German Bight triangle are obvious for the whole time period in the NCEP/NCAR data. In the median and the 95th percentile series no significant trend is visible.

In conclusion, it is possible to calculate the geostrophic wind speed over the German Bight and the south-western Baltic Sea by using observational and reanalyses data to create a time series from 1965 to 2012 for these coastal areas. The time series of the 95th percentile and the median of observational data do not show a significant trend during these time periods for all three triangles. Also, there is no trend recognized in the reanalysis data. What is recognizable is a spread between the 95th percentile of the geostrophic wind of the North Sea and the Baltic Sea triangles calculated from the CoastDat2 dataset, which indicates much higher wind speeds at the German Bight than at the south-western Baltic Sea. These spreads can also be seen in the geostrophic wind speed calculated by the NCEP/NCAR data and for the time period from 1984 to 2004 for the geostrophic wind speed calculated by the observational data. Some specific peaks (e.g in 1882, 1990 and 1956) can be found in all calculations of the geostrophic wind from different datasets. These consistancies gives the possibility to use different station positions (e.g. signal stations) for the calculation of the geostrophic wind speed using triangles and this leads to a possibility of an extension of the time series.

4.3 Signal Station Wind Data

In addition to historical SLP data, signal station data also provides information on the wind statistics at the German coastlines for several decades. At Travemünde station (Baltic Sea coast) wind observation data over a time period of 120 years are aquired. This is the longest time series of wind data, which was observed at signal stations. These wind data are analyzed in the following section.
For the trends analysis and the evaluation of the potential for trend in storm surges at the German Bight it is important to not only investigate wind speed, but also wind direction trends. Therefore, the change of wind direction of four representative stations along the German Bight and southern Baltic Sea coastline are analyzed.
Wind force, wind direction and their changes over Europe are highly influenced by the NAO. The NAO and its indices, as well as the change of wind force and wind direction, is analyzed in the next section.

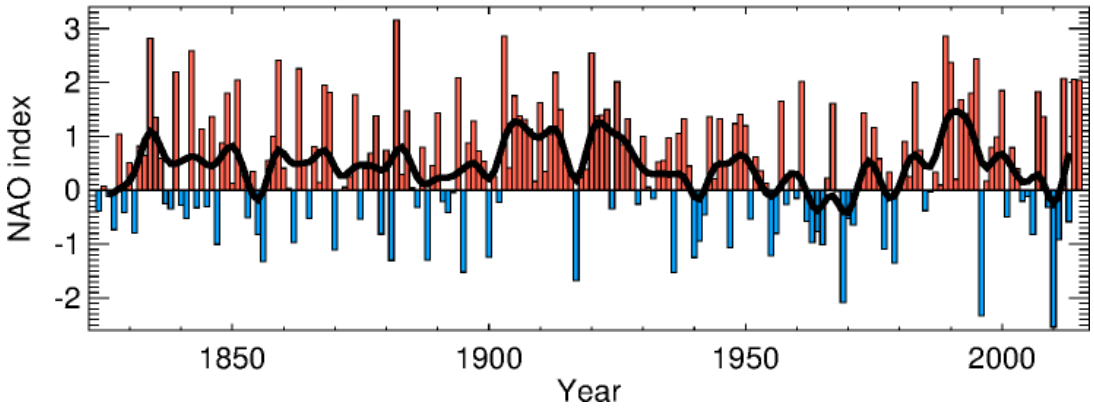

Figure 4.4.: Time series of the winter (DJFM) NAO-Index. The black line is the smoothed curve of 10 years (Source: CRU (2016) and Jones et al. (1997)).

4.3.1 The NAO-Index

The NAO describes a major part of the variability in the northern hemisphere atmosphere and the influences on its climate. The difference in normalized SLP over Gibraltar and the South-West of Iceland causes changes and this is associated with variabilities in air temperature, precipitation and wind force and direction over Europe. The winter season indicates strongest interdecadal variability. The time series of the index, back to 1823, indicates the variability of strength of the NAO in the winter months (December to March) and is figured in Fig. 4.4 (Jones et al., 1997). A positive NAO-index means a strong difference between the SLP over Gibraltar and Iceland. The air temperature in winter in North and mid-Europe is relatively high, because of the advection of warm air from the North Atlantic, which is linked to a positive NAO-Index. It also leads to strong westerly winds in Europe. A relative low air temperature over Europe is related to a negative NAO-index. The air temperature gets lower because of the advection of cold air from Siberian latitudes. It also implies a year with a weak gradient of SLP between Gibraltar and Iceland, which indicates relatively weak wind forces and several predominant wind directions. The influences of the NAO to the wind field in West and mid-Europe go along with the variability in the surface water temperature (Hurrel and van Loon (1997) and Jacobeit et al. (1998)).
Fig. 4.4 shows a decreasing trend from about 1900 to 1960, and an increasing trend up to 1990. Significant maxima are in 1835, 1882, 1903 and 1989 and significant minima in 1917, 1969 and 1996.

4.3.2 Change of Wind force over 120 years

For the signal station Travemünde, at the south-western Baltic Sea coast, wind observations for over 120 years exist. The time series of the 95th percentile (red line), the 90th percentile (blue line) and the median (black line) are shown in Fig. 4.5. The median of the wind force of Travemünde station shows the values 2 Bft, 3 Bft and 4 Bft. Obviously there are the nearly yearly variations of 2 Bft and 3 Bft of the wind force of the median between 1941 and 1963, and variations of 3 Bft and 4 Bft between 1978 and 1999. These partly strong variations suggest on the one hand an inhomogeneity of the time series. On the other hand these variations could be random because of a median very near 2.5 Bft. The 95th and 90th percentiles show higher values from about 1878 to 1940, to respectivly 1930. The 95th percentile of wind force also show higher values between about 1975 and 1999. During these two time periods with higher wind force values of the 95th percentile the NAO-index also shows mostly a positive index, which is also a factor related to high wind forces in Europe.
The distribution of the wind force of Travemünde station in Fig. 4.6 shows an observation without 0 Bft between about 1965 and 1999. This assumes a higher median for the time period of 1978 and 1999 and therefore suggests the possibility of an overestimation of the wind force. The opposite assumption is true for the lower part of the median. The reason for such inhomogeneities could be because of a change in the observer, who estimated the wind forces in different ways.
To get a better idea of what this means for the possibility of storms, the total number of stormy days for the months October, November, December, January, February and March (ONDJFM) is shown in Fig. 4.7. The number of days for each month and each year for the Travemünde station with a wind force of more than 8 Bft are counted and displayed. The very light blue boxes indicate that there are no days with a wind force of more than 8 Bft. Dark boxes indicate a high number of storms, up to 22 days in December 1921. The results for the months January, February and March represent the following year. There are two periods with obviously more stormy days in the first half of the total period. The first is seen in the beginning of the time period, between about 1887 and 1889, and a second between about 1915 and 1930. On the other hand, a time section with obviously less stormy months is evi-

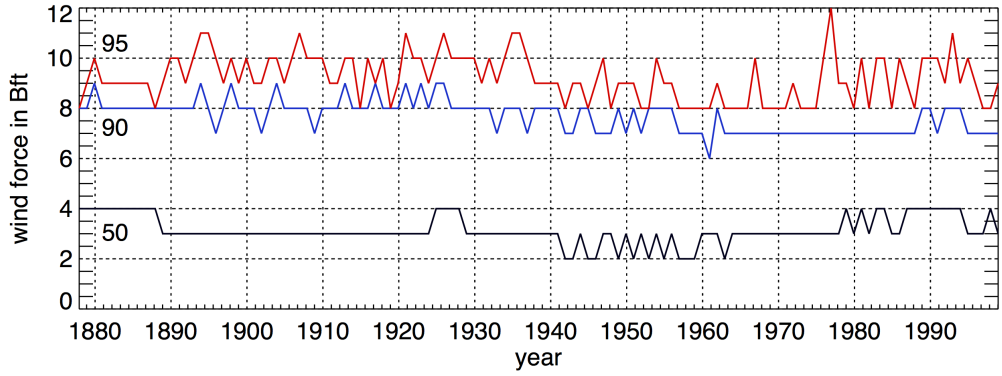

Figure 4.5.: Time series of the 95th percentile (red), the 90th percentile (blue) and the median of the wind force at Travemünde station from 1878 to 1999.

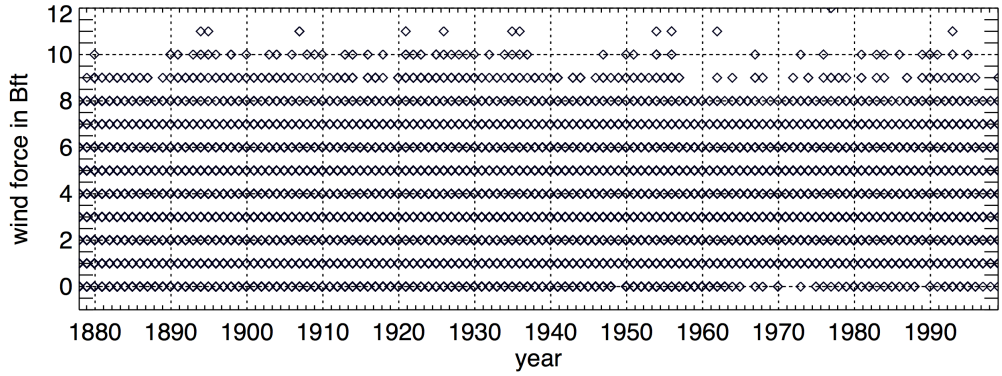

Figure 4.6.: Time series of daily wind force in Bft of signal station Travemünde from 1878 to 1999.

dent (between about 1955 and 1999) in the second half of the time period. A comparison with the NAO-index reveals that the two periods with high numbers of storm days match with a positive NAO-index and the part with low numbers of storm days between about 1955 and 1980 match with a negative NAO-index period. The analysis of the number of storm days is quite useful in respect to trend analysis of storminess.

In consideration of the possible inhomogeneity of the wind data, the quality of the changing number of stormy days is estimated by the distribution of storm frequency. The distribution of the absolute frequency of the wind force of three different months in three different years are displayed for the Travemünde station in Fig. 4.8. The red bars show the frequency of wind force from January 1971 with a low number of stormy days. The blue and

black bars show the frequency of wind force from January 1884 and December 1921, respectively with a high number of stormy days. It is evident that the maximum of the distributions of the months with no stormy days (red) is shifted to the lower wind force and the maximum number of the distribution of high monthly storm numbers (blue) are shifted to the higher wind force.

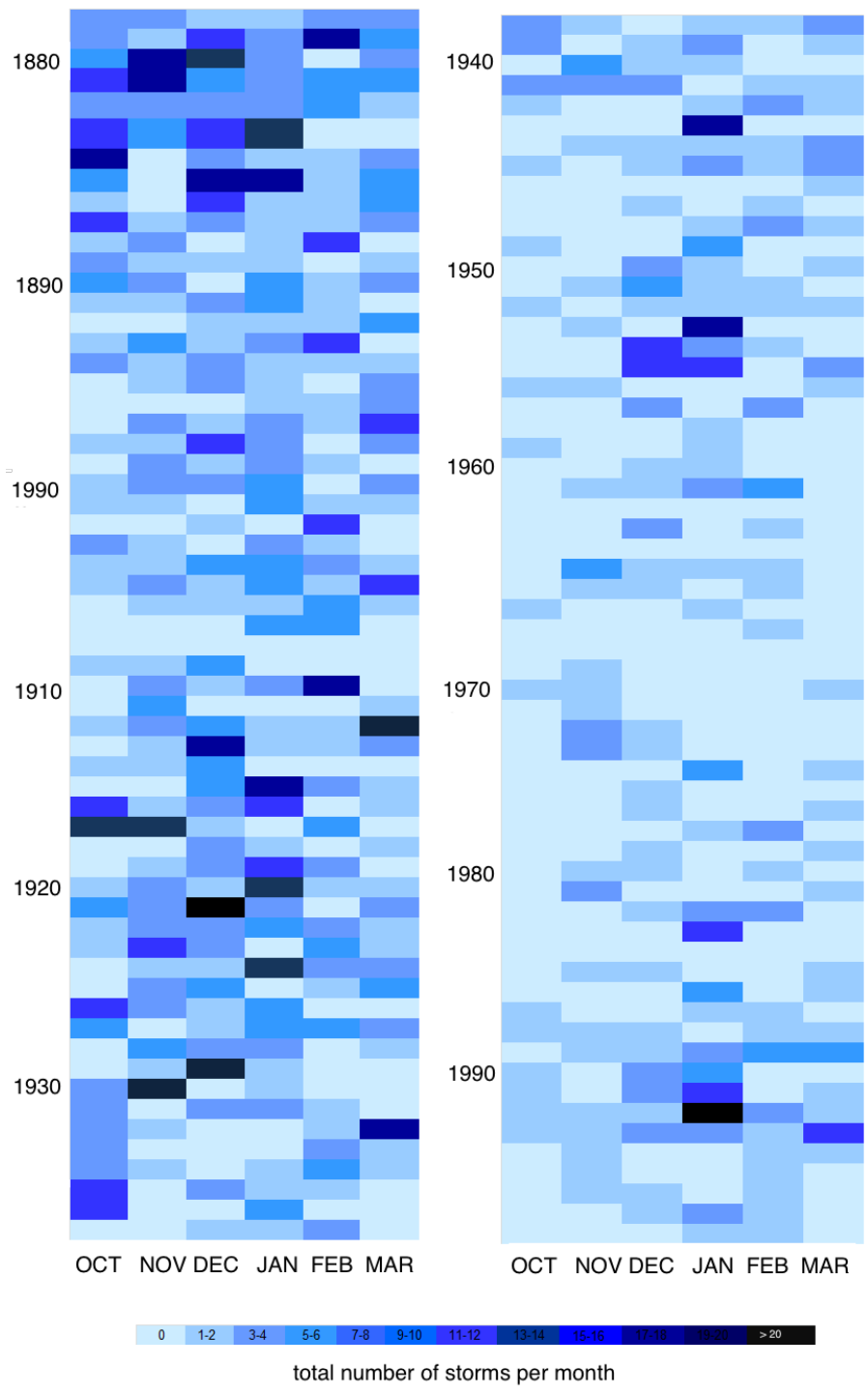

Figure 4.7.: Total number of storm days in Travemünde between 1878 and 1999 for October, November, December, January, February and March. The light blue boxes are no or low numbers of storm days and the dark boxes are months with high numbers of storm days up to 22 days in October 1921.

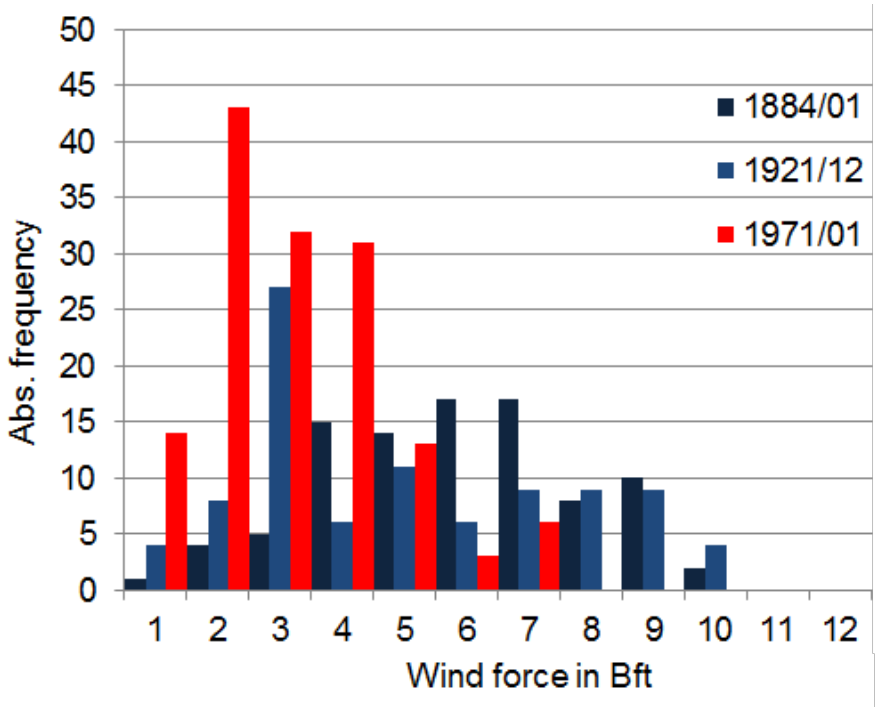

Figure 4.8.: Distribution of absolute frequency of the wind force of December, January and February at the signal station Travemünde. The frequency of wind force from January 1971/01 with a low number of stormy days, the blue and black bars show the frequency of wind force from January 1884 and December 1921 with a high number of stormy days.

4.3.3 Change of Wind Direction

The wind direction is an important parameter, in combination with the wind force, in regard to the potential for storm surges at the German coasts. The change of wind direction for five stations, two at the German Bight coast (Emden and Bremerhaven) and three at the Baltic Sea coast (Flensburg, Kiel and Travemünde) is analyzed. The Emden station observed wind direction data between 1887 and 1943, as well as the stations in Bremerhaven and Flensburg. Wind direction information for 57 years between 1897 and 1940 are available from the Kiel station and between 1878 and 1999 for Travemünde station.

Fig. 4.9 shows the relative numbers of the wind direction for Emden station between 1887 and 1943. On the left, the relative numbers of wind direction are shown for the whole time period. The left graph shows a more smooth

distribution of the wind direction between 1887 and 1914 than in the later part, caused by different used wind roses. Until 1914 the 8-part wind rose was used, later the 16-part wind rose. To provide a useful comparison of the relative number of wind direction, these two periods are separated. The right graph shows the relative number of this two separated time periods. The period between 1887 and 1914 is regarded separately from the later part with its own relative numbers. For the whole time section, it is obvious that a wind direction of 225° is the predominant direction. Between 1925 and 1930 in particular, a high number of winds in the direction of 225° is obvious. This goes in accordance with a positive NAO-Index during this time period. A relative high number in wind direction of 90° or a relatively even distribution over all wind directions can be found in 1887 or 1932, which are evident to a negative NAO-Index. The distribution of the relative number of wind directions over a time period gives us information about the negative and the positive NAO-Index in regard to the wind direction.

Fig. 4.10 shows the relative numbers of the wind direction for Bremerhaven station between 1887 and 1941. On the left, the numbers of wind direction, over the whole time period up to 1941, and on the right, the numbers of wind direction separated in two parts, because of differently used wind roses during observation. From 1887 to 1902 and between 1939 and 1941, the 8-part wind rose and between 1905 and 1939 the 16-part wind rose was used. The different used wind roses lead to a predominant wind direction of 225° from 1887 to 1905 and between 225° and 270° from 1904 to 1940, caused by a higher resolution of the wind rose. A relatively predominant wind directions of 225° can be found for the year 1882, the time period between 1904 and 1917 and between 1920 and about 1930. This years are evident to a positive NAO-Index. A higher numbers in the easterly wind directions of more even distribution can be found for the years 1885, 1904, 1917, and the period between 1939 and 1941. This years are evident to a negative NAO-Index.

Fig. 4.11 shows the relative numbers of wind direction for the Kiel station in the left and Flensburg station on the right. These stations are located at the Baltic Sea coast. The time series of Kiel station begins in 1897 and ends in 1940. At Flensburg station the wind direction data were measured from 1887 to 1941. Over both whole time periods, the observation is mostly given with

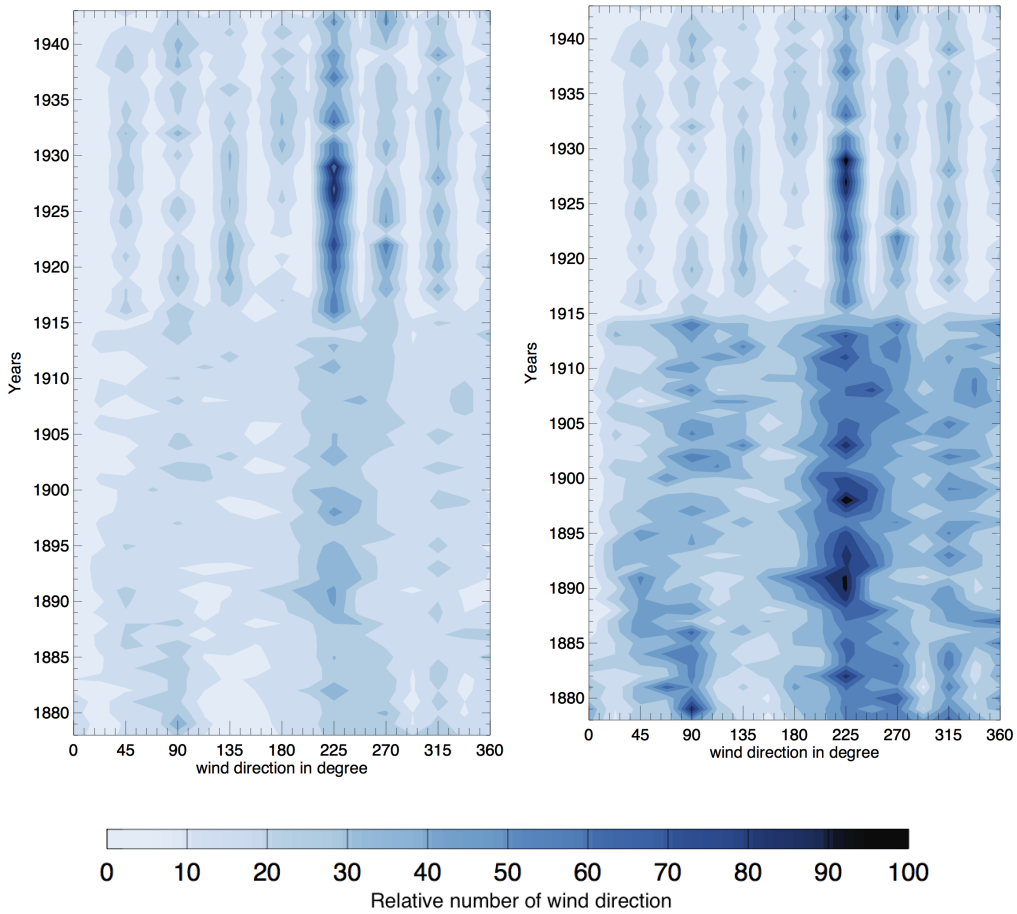

Figure 4.9.: Variations of the relative numbers of wind direction for the Emden station from 1878 to 1943. On the left, the distribution of the relative numbers of wind direction for the whole time period and on the right, the distribution of wind direction for separated relative numbers for the periods (1878-1914, 1915-1943).

a 8-part wind rose. For Kiel station two main wind directions are obvious. These are 225° and 315°. There are high numbers of a 315° wind direction between 1917 and 1938. A predominant high number of wind direction 225° can be found between 1904 and 1917. This years are evident to a significant positive NAO-Index. In 1900, 1904, 1917 and 1932 an even distribution of numbers of wind direction for Kiel station can be found, which matches the years with a negative NAO-Index.

The Flensburg station (4.11, right) shows high numbers of wind direction of 225° and 270° during the time period from 1887 to 1941. The high numbers of 0° between 1915 and 1920 are caused by giving the number 0, in case of a wind force of 0 Bft. For the time period from 1904 to 1916 the predominant

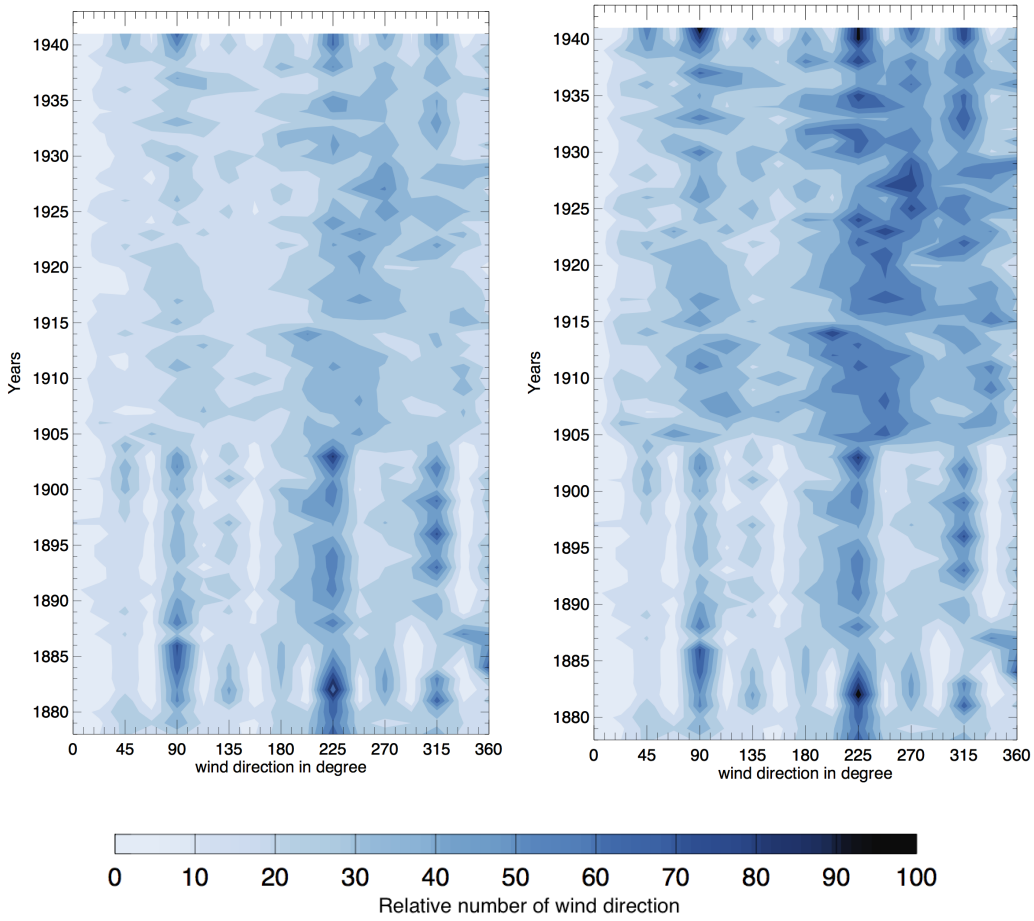

Figure 4.10.: Variations of the relative numbers of wind direction from Bremerhaven station from 1878 to 1943. On the left, the distribution of the relative numbers of wind direction for the whole time period and on the right, the distribution of the relative numbers of wind direction for two time sections (1878-1904, 1905-1941).

wind directions of 225° and 270° are obvious. For this years a positive NAO-Index is evident. In the years 1900, 1917 and 1927 a more even distribution of the wind direction numbers is obvious. This years matches the negative NAO-Index

The longest time series of wind observation data from signal stations in Travemünde is figured in 4.12. From 1878 to about 1915, a different wind rose was used than for the other part of the time series. This is evident by the more even distribution over all wind directions. It is obvious that the predominant wind directions for the Travemünde station are 225° and 270° during almost the entire time period from 1878 to 1999. In 1917 and in the time period between 1950 and 1954 a relative high number of a 90° is obvious. These years

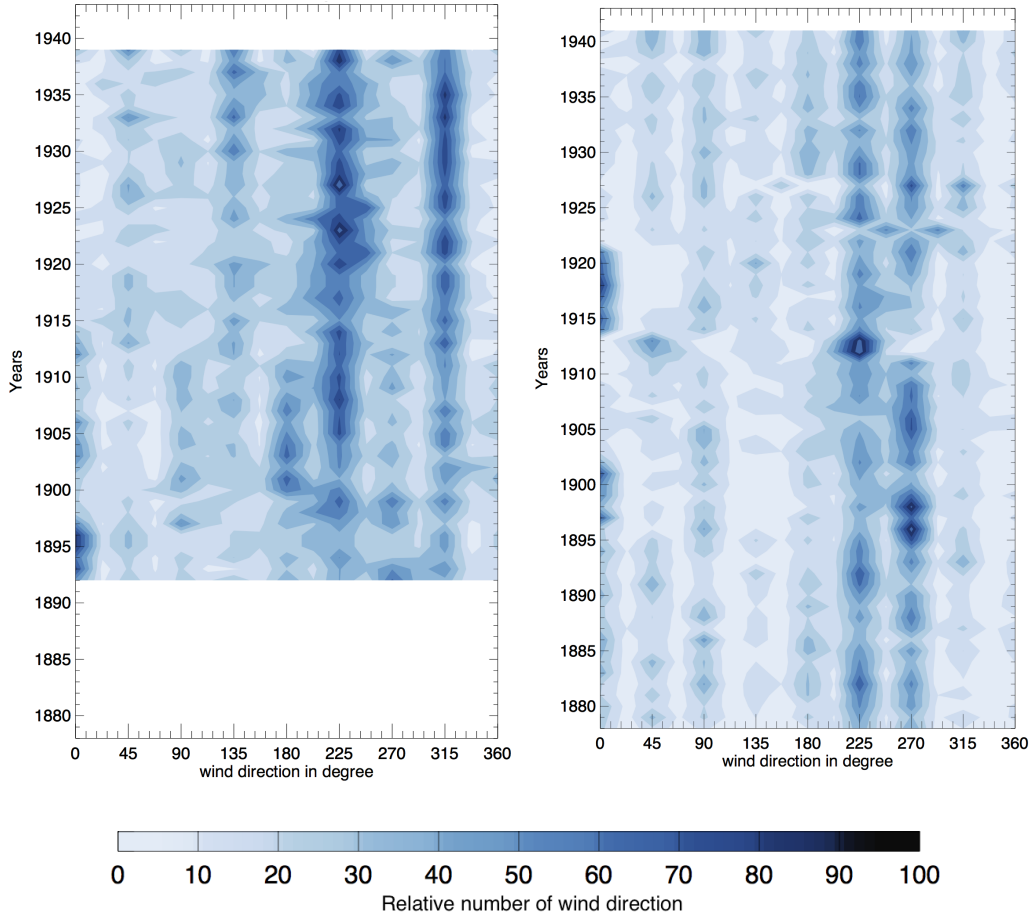

Figure 4.11.: Variations of the relative numbers of wind direction for the Kiel station on the left from 1892 to 1939 and on the right, the relative numbers of wind direction from Flensburg station from 1878 to 1941.

are evident to a negative NAO-Index. In addition a higher number of westerly wind direction can be recognized between 1982 and 1994. This matches the positive NAO-Index, which is associated with wind from westerly directions.

The distributions of the relative number of wind directions for five stations at the German coast show all a predominant westerly wind direction of about 225°. In the wind direction data of Emden, Bremerhaven, Kiel, Flensburg and Travemünde station typical years with a positive or negative NAO-Index are obvious.

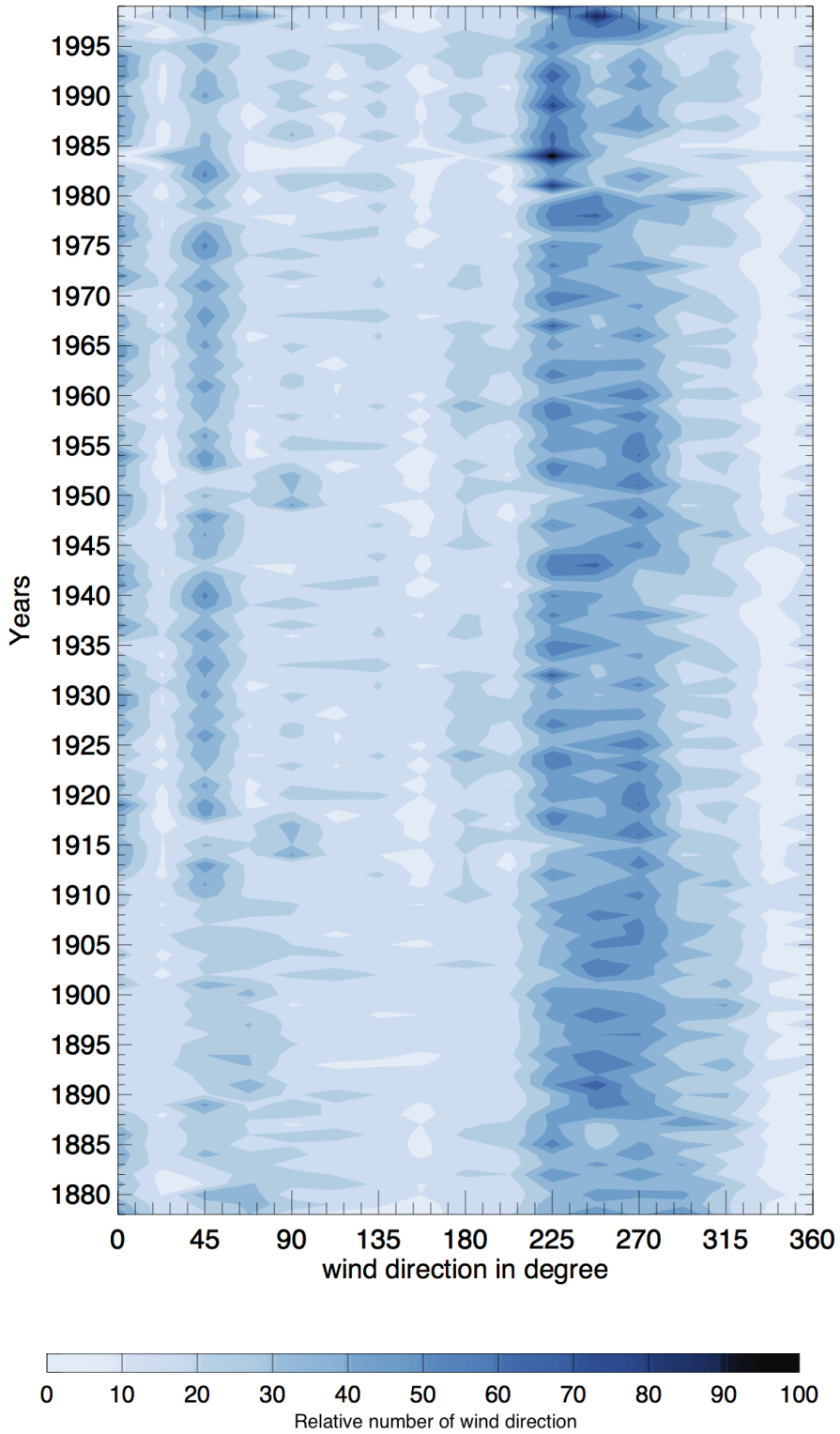

Figure 4.12.: Variations of the relative numbers of wind direction from Travemünde station with the predominant wind directions of 225° and 270° from 1878 to 1999.

4.4 Conclusion

The calculations of the geostrophic wind from observation and reanalysis data over the German Bight and the southern Baltic Sea do not show a significant trend during the time period from 1965 to 2012. Observation and reanalysis data show some peaks during the time periods, which are mostly evident in all calculated time series of the geostrophic wind. An extension of the time series with signal station data is aspired after. The comparison of the time series of the geostrophic wind of observation data with the geostrophic wind of reanalysis data show that also the time series for the NCEP/NCAR data with a low resolution are in accordance in specific peaks with observation data. This implies that an extension of the time series by signal station data in the spatial surrounding of the used data is possible. Also, the SLP data itself can give an input to reanalysis data sets and can improve the reanalysis. The wind data from signal stations also gives a benefit to the evaluation of storminess at the German Bight and the southern Baltic Sea. It is shown that the high percentiles for the wind force of the Travemünde station can be linked to the NAO-index. In consideration of assumed inhomogeneities of the wind data from the Travemünde station, also the change in numbers in stormy days from 1887 to 1999 can be linked to the NAO-index. The time series of the relative numbers of wind directions from five signal stations along the German coastline shows, in the comparison to the NAO-index, matching results. The signal station wind data are also quite useful for long-term scientific analysis. Considering an inhomogeneity of the wind data, a trend analysis is not given until a justified homogenization.

5 Conclusion and Outlook

Signal stations were built in the late 19th century along the German coast to warn the coastal population of severe storms. In addition to the storm warnings, atmospheric observations were done at the signal stations between 1878 and 1999. The main topic of this thesis is the assesment of meteorological observation data of signal stations in terms of their usefulness for investigations in the long-term trend analysis of storminess. In this context, the SNHT is used for the homogeneity testing and SLP data. For trend analyses of storminess, the geostrophic wind is calculated from SLP triangles. In addition to observational data, data of two reanalyses are used (coastDat2 and NCEP/NCAR).
In this chapter the main results of this thesis will be summarized and the main research questions will be answered and discussed. An outlook for future investigations on the signal station data and their contribution to future scientific research, in regard to trend analyses of storminess, is given at the end of this chapter.

5.1 Conclusion

In the first step, an introduction to the history of signal stations of the German Naval Observatory (Deutsche Seewarte) and their functions is given and the existence of atmospherical observation data is described.
Relating to the research question, whether the wind and SLP data of signal stations are homogenious in time and space, the quality of the signal station data is tested considering two different aspects: Formal uncertainties and homogeneity.
The formal uncertainties are checked by the *validat* routine. Additional to formal uncertainties, climatological and repetitive uncertainties are detected. The maximal number of formal mistakes in the wind and SLP data of 15 selected signal stations is 0.1 %. 0.3 % of the proved data show climatological uncertainties and the repetitive uncertainties topped out with a maximum of 3 %. Observation methods in the beginning of the 20th century to the relatively high number in repetitive uncertainties, especially for wind observa-

tions. The testing of homogeneity of the signal station data, as the second consideration, is done in two ways. Firstly, the spatial homogeneity is checked by the analysis of two historical storm surges in 1906 (in the German Bight) and in 1913 (at the southern Baltic Sea). The signal station wind and SLP data extend the monitoring network during the occurence of the storm surges. In addition to the weather observation of the Deutsche Seewarte, which flow into the daily weather forecast, the signal station data extend this network. For the storm surge in 1906 at the German Bight, the signal station data doubled and for the storm surge in 1913 the signal station data decupled the network. The wind direction and wind force show, for both storm surges, an agreement with the routine stations of the Deutsche Seewarte. It is also possible to improve the pressure field of the storm surge situations by the SLP data of the signal stations. It has to be noted that a high number of signal station SLP data do not match the air pressure field exactly. The reason for this could be a missing reduction to NHN. In conclusion, it can be said that the signal station wind data are homogeneious in space and can be used for extreme event analyses and the SLP data have to be proved in their reduction to NHN.
In the second step, the chronological homogeneity is tested for the SLP data in chapter 3. The detection of inhomogeneity of the time series of SLP data is done by the SNHT with data from 15 signal stations. The results show that eleven of fifteen time series point out to at least one non-homogeneity. The inhomogeneity appear for each station in different years. The reason for the occurrence of inhomogenities at SLP time series could be due to the change in observers. The metering of the SLP could be done incorrectly or at a different point of time. In addition, a recalculation from mmHg to hPa is possible and perhaps not all data are reduced to NHN. There is no information about the change of observers or instruments. The possibility of a homogenization of the SLP data, observed at signal stations from 1910 to 1939 is also shown.

Relating to the second research question, whether the signal station data are worthwhile for scientific research in regard to long-term trend analysis of storminess at the German coasts, the time series of the geostrophic wind are calculated and secondly, long-term wind observations of signal stations are analyzed. These analyses are illustrated in chapter 4.
The calculation of the geostrophic wind is done for three triangles, each by observational and reanalysis data. There are two reasons for using SYNOP-

data as observational data, instead of signal station data. Firstly, the construction of triangles with time series of the same length was not available for the German Bight at the time of calculation because of the current ongoing digitization of all signal station data. Secondly, for a comparison with reanalysis data the time series of SLP data from signal stations is too short and ends in 1939. The results of the comparison of time series of the geostrophic wind of SYNOP-data, observational data and reanalyses data show no significant trend for the high percentiles of the geostrophic wind. Additionally, it is shown that the signal station SLP data could extend the time series for the geostrophic wind of triangles back to 1878.
The second step of evaluation of long-term variabilities in storminess at the German coasts are shown by the analysis of wind data at the Travemünde station. The high percentiles of the wind force and the variability of numbers of stormy days can be linked to the NAO-index, as well as to the variability of wind direction of further signal stations. A trend analysis is not available until a justified homogenization of the wind force data is possible.

5.2 Outlook

This thesis discloses some aspects for further investigations of signal stations. The main aim in further investigations should be a set up of the signal station data as a complete dataset, including metadata. Therefore, all signal station data should be proved on uncertainties and inhomogeneity. In detail investigations on the reduction of the SLP data to NHN are necessary after digitization for a scientific analysis. Furthermore, investigations into the homogenization of the signal station data are needed. The homogenization of SLP data should be done with time series of monthly means, instead of yearly means. The time series of yearly means are too short to assess several points of inhomogeneity during the time period. The assessment of monthly means would lead to a more accurate homogenization. More research should be done on the homogenization of wind force time series, because of missing studies in the literature.
For the evaluation of storminess, the extension of time series of the geostrophic wind should be excecuted. What should be considered is the calculation of the geostrophic wind for more triangles in the southern Baltic Sea. Therefore, a collaboration with other Scandinavian weather institutes is would be ad-

vantageous.
A further interesting research question is the assessment of the quality of the storm warnings of the signal stations.

List of Symbols and Abbreviations

Abbreviations

20CR Twentieth Century Reanalysis

ACRE Atmosphere Circulation Reconstructions over the Earth

a.s.l. above sea level

Bft Beaufort

BSH Bundesamt für Seeschifffahrt und Hydrografie

BUFR Binary Universal Form for the Representation of meteorological data

CET Central European Time

CliSAP Integrated Climate System Analysis and Prediction

DFG Deutsche Forschungs Gesellschaft

DKRZ Deutsches Klimarechenzentrum

DMI Danish Meteorological Institute

DWD Deutscher Wetterdienst

ECWMF European Centre for Medium-Range Weather Forecast

GeoInfoDBw Geoinformationsdienst der Bundeswehr

HZG Helmholtz Zentrum Geesthacht

ICOADS International Comprehensive Ocean-Atmosphere Data Set

ISTI International Surface Temperature Initiative

MARNET Marine Environmental Monitoring Network

NAO North Atlantic Oscillation

NCAR National Center for Atmospheric Research

NCEP National Center for Environmental Prediction

NHN Normal Height Null

NOAA National Oceanic and Atmospheric Administration

SASSCAL South African Science Service Centre for Climate Change and Adaptive Land Management

SICSS School of Integrated Climate System Sciences

SLP Sea Level Pressure

SNHT Standard Normal Homogeneity Test

WMO World Meteorological Organisation

WWII Second World War

Greek Symbols

μ_1	Theoretical mean level of standardized differences before a possible shift
μ_2	Theoretical mean level of standardized differences after a possible shift

Latin Symbols

a	Last year before possible shift
i	Time unit index
n	Number of values in a time series
q	Estimated difference of candidate time series and reference series
$\overline{q}$	Mean value of estimated difference of candidate and reference series
z_i	Difference of candidate series and weighted average from reference series
H_0	Null hypothesis
H_1	Alternative hypothesis
K	Kelvin
N	Gaussian distribution
S_q	Standard deviation
T	A test value for a single shift test
T_{max}	A test value for single shifts. Maximum of T
T_{95}	Critical values at 95 per cent significance
Z_1	Estimated mean level of a series of differences before a possible shift
Z_2	Estimated mean level of a series of differences after a possible shift

Bibliography

H. Alexandersson. A Homogeneity Test Applied to Precipitation Data. *Journal of Climatology*, 6:661–675, 1986.

H. Alexandersson and A. Moberg. Homogenization of Swedish Temperature Data. Part I: Homogeneity Test for Linear Trends. *International Journal of Climatology*, 17:25 – 34, 1997.

H. Alexandersson, H. Tuomenvirta, T. Schmith, and K. Iden. Trends of Storms in NW europe Derived from an Updated Pressure Data Set. *Climate Research*, 14:71–73, January 2000.

R. Allan, G. Compo, and J. Carton. Recovery of Global Surface Weather Observations for Historical Reanalyses and International Users. In *AGU*, volume 92, 2011.

L. Bärring and K. Fortuniak. Multi-indices Analysis of Southern Scandinavian Storminess 1780-2005 and Links to Interdecadal Variations in the NW Europe-North Sea Region. *International Journal of Climatology*, 29:373–384, 2009.

L. Bärring and H. von Storch. Scandinavian Storminess Since About 1800. *Geophysical Research Letters*, 31:1790–1820, 2004.

M. Beniston and Coauthors. Future Extreme Events in European Climate: An Exploration of Regional Climate Model Projections. *Climate Change*, 81: 71–95, 2007.

S. Brönnimann, O. Martius, H. von Waldow, C. Welker, J. Luterbacher, G. P. Compo, P. Sardeshmukh, and T. Usbeck. Extreme Winds at Northern Midlatitudes Since 1871. *Meteorologische Zeitschrift*, 21:13–27, 2012.

V. Brownrigg. San francisco's telegraph hill. URL `http://www.wildirisdesign.com/cis78.11/`.

M. Brunet and P. Jones. Data Rescue Initiatives: Bringing Historical Climate Data Into the 21st Century. *Climate Research*, 47:29–40, 2011.

K. Bülow, A. Ganske, H. Heinrich, S. Hüttl-Kabus, B. Klein, H. Klein, J. Möller, G. Rosenhagen, N. Schade, and B. Tinz. Comparing Meteorological Fields of the ENSEMBLES Regional Climate Models with ERA.40-Data Over the North Sea. Technical Report 21, KLIWAS, 2013.

J. Cappelen. Technical Report 13-02 - Denmark-DMI Historical Climate Data Collection 1768-2012. Technical Report 13-02, Danish Mteorological Institute, Copenhagen, 2013.

D. Carter and L. Draper. Has the North-East Atlantic Become Rougher? *Nature*, 332:494, 1988.

P. Ciavola, O. Ferreira, P. Haerens, M. V. Konigsveld, C. Armaroli, and Q. Lequex. Storm Impacts Along European Coastlines. Part 1: The Joint Effort of the MICORE and ConHAZ Projects. *Environmental Science and Policy*, 14:912–923, 2011.

G. P. Compo, J. Whitaker, P. Sardeshmukh, N. Matsui, R. Allan, X. Yin, J. B.E. Gleason, R. Vose, G. Rutledge, P. Bessemoulin, S. Brönnimann, M. Brunet, R. Crouthamel, A. Grant, P. Groisman, P. Jones, M. Kruk, A. Kruger, G. Marshall, M. Maugeri, H. Mok, O. Nordli, T. Ross, R. Trigo, X. Wang, S. Woodruff, and S. Worley. The Twentieth Century Reanalysis Project. *Quarterly Journal of the Royal Meteorology Society*, (137):1–28, 2011.

V. Conrad and C. Pollak. *Methods in Climatology*. Harvard University Press, 1950.

CRU. Tim Osborn: NorthAtlantic Oscillation Index Data, May 2016. URL `https://crudata.uea.ac.uk/~timo/datapages/naoi.htm`.

S. Cusack. A 101 Year Record of Windstorms in the Netherlands. *Climate Change*, 116:693–704, 2013.

D. Dee, S. Uppala, A. Simmons, P. Berrisford, P. Poli, S. Kobayashi, U. Andrae, M. Balmaseda, G. Balsamo, P. Bauer, et al. The era-interim reanalysis: Configuration and performance of the data assimilation system. *Quarterly Journal of the royal meteorological society*, 137(656):553–597, 2011.

P. Domonkos, V. Venema, I. Auer, O. Mestre, and M. Brunetti. The Historical Pathway Towards More Accurate Homogenisation. *Advances in Science and Research*, 8:45–52, 2012.

M. Donat, G. Leckebusch, J. Pinto, and U. Ulbrich. European Storminess and Associated Circulation Weather Types: Future Changes Deduced from a Multi-Model Ensemble of GCM Simulations. *Climate Research*, 42:27–43, 2010.

DWD. *Dienstanweisung für die Sturmwarnungsstellen an der deutschen Küste*. Deutscher Wetterdienst - Seewetteramt, Hamburg, 1955.

DWD. *Dienstanweisung für die Sturmwarnungsstellen an der deutschen Küste*. Deutscher Wetterdienst - Seewetteramt, Hamburg, 1969.

DWD. Observation Network of the DWD, 2016a. URL `http://www.dwd.de/DE/derdwd/messnetz/bodenbeobachtung/bodenbeobachtungen_node.html`.

DWD. The Signal Stations Along the North and Baltic Sea Coasts, August 2016b. URL `http://www.dwd.de/EN/ourservices/signal_stations/signalstationen.html`.

D. Easterling and T. Peterson. Techniques for Detecting and Adjusting for Artificial Discontinuities in Climatological Time Series: A Review. In *Fifth International Meeting on Statistical Climatology*, pages J28–J32, 1992.

ET. Lloyd's Signal Station, 2016. URL `http://www.engineering-timelines.com/scripts/engineeringItem.asp?id=1048`.

D. Etling. *Theoretische Meteorologie*. Springer Verlag, Berlin, Heidelberg, New York, 3 edition, 2008.

F. Feser, O. K. M. Barcikowska, F. Schenk, R. Weisse, and L. Xia. Storminess Over the North Atlantic and Northwestern Europe -A Review. *Quarterly Journal of the Royal Meteorology Society*, 141:350–382, 2015.

B. Geyer. High-Resolution Atmospheric Reconstruction for Europe 1948-2012: Coastdat2. *Earth System Science Data*, 6(147-164), 2014.

G. Gönnert, S. Dube, T. Murty, and W. Siefert. *Global Storm Surges*. Die Küste, 2001.

R. Heinkelmann, J. Boehm, and H. Schuh. *Homogenization of Surface Pressure Recordings and its Impact on Long-Term Series of VLBI Tropospheric Parameters*. NA, 2005.

HKO. The Day and Night Signals. URL http://www.hko.gov.hk/wservice/tsheet/pms/tc_signal_e.htm.

T. Hofherr and M. Kunz. Extreme Wind Climatology of Winter Storms in Germany. *Climate Research*, 41:105–123, 2010.

J. Hurrel and H. van Loon. Decadal Variations in Climate Associated with the North Atlantic Oscillation. *Climate Change*, 36:301–326, 1997.

HZG. CoastDat, 2016. URL http://www.coastdat.de/about_us/index.php.

J. Jacobeit, C. Beck, and A. Philipp. *Annual to Decadal Variability in Climate in Europe.* Würzburg, 1998.

J. Jensen and S. Müller-Navarra. Storm Surges of the German Coast. *Die Küste*, 74:92–124, 2008.

P. Jones, T. Jonsson, and D. Wheeler. Extension to the North Atlantic Oscillation Using Early Instrumental Pressure Observations from Gibraltar and South-West Iceland. *International Journal of Climatology*, 17:1433–1450, 1997.

P. Jones, K. Trenberth, P. Ambenje, R. Bojariu, D. Easterling, T. Klein, D. Parker, J. Renwick, M. Rusticucci, B. Soden, et al. Observations: Surface and Atmospheric Climate Change. *IPCC, Climate change*, pages 235–336, 2007.

Kaiho. For the Safety Navigation in Japanese Coastal Waters. URL http://www.kaiho.mlit.go.jp/syoukai/soshiki/toudai/navigation-safety/en/pdf/english.pdf.

E. Kalnay, M. Kanamitsu, R. Kistler, W. Collins, D. Deaven, L. Gandin, M. Iredell, S. Saha, G. White, J. Woollen, Y. Zhu, M. Chelliah, W. Ebiuzaki, W. Higgins, J. Janowiak, K. Mo, C. Ropelewski, J. Wang, A. Leetma, R. Reynolds, R. Jenne, and D. Joseph. The NCEP/NCAR 40-Year Reanalysis Project. *Bulletin of the American Meteorological Society*, 77(3):437–471, 1996.

F. Kaspar, B. Tinz, H. Mächel, and L. Gates. Data Rescue of National and International Meteorological Observations at Deutscher Wetterdienst. *Advances in Science and Research*, 12(1):57–61, 2015.

M. Khaliq and T. Quarda. On the Critical Value of the Standard Normal Homogeneity Test (SNHT). *International Journal of Climatology*, 27:681–687, 2007.

O. Krüger and H. von Storch. Evaluation of an Air Pressure-Based Proxy for Storm Activity. *Journal of Climate*, 24:2612–2619, 2011.

O. Krüger and H. von Storch. The Informational Value of Pressure-Based Proxies for Past Storm Activity. *Journal of Atmospheric and Oceanic Technology*, 29:569–580, 2012.

O. Krüger, F. Schenk, F. Feser, and R. Weisse. Inconsistencies between Long-Term Trends in Storminess Derived from the 20CR Reanalysis and Observations. *Journal of Climate*, 26:868–874, 2013.

Lloyds. Lloyd's Register of Shipping. 1907.

H. Luthardt and L. Hasse. On the Relationship between Surface and Geostrophic Wind in the Region of the German Bight. *Contribution to Atmospheric Physics*, 54:222–237, 1981.

H. Luthardt and L. Hasse. The relationship between pressure field and surface wind in the german bight area at high wind speeds. In *North Sea Dynamics*, pages 340–348. Springer, 1983.

L. Minola, C. Azorin-Minola, and D. Chen. Homogenization and assessment of observed near-surface wind trend across sweden, 1956-2013. *Journal of Climate*, 29:7397–7415, 2016.

M. Petersen and H. Rohde. *Sturmflut. Die großen Fluten an den Küsten Schleswig-Holsteins und in der Elbe*. Karl Wachholz Verlag, 1977.

T. Peterson, D. Easterling, T. Karl, P. Groisman, N. Nicholls, N. Plummer, S. Torok, I. Auer, R. Boehm, D. Gullett, L. Vincent, R. Heino, H. Tuomenvirta, O. Mestre, T. Szentimrey, J. Salinger, E. J. Förland, I. Hanssen-Bauer, H. Alexandersson, P. Jones, and D. Parker. Homogeneity Adjustments of In Situ Atmospheric Climate Data: A Review. *International Journal of Climatology*, 18:1493–1517, 1998.

S. Ribeiro, J. Caneta, and A. Costa. Review and Discussion of Homogenisation Methods for Climate Data. *Physics and Chemestry of the Earth*, 2015.

G. Rosenhagen and I. Bork. Rekonstruktion der Sturmwetterlage vom 13. November 1872. In K. für Forschung im Kuesteningenieurwesen, editor, *Die Kueste - Archive for Research and Technology on the North Sea and Baltic Coast Archive for Research and Technology on the North Sea and Baltic Coast*, volume 75, page 271. MUSTOK - Modellgestütze Untersuchungen zu Extremen Sturmflutereignissen an der Deutschen Ostseeküste, 2009.

H. Schmidt. On the Variation of the Geostrophic Wind from 1876 to 1989 in the German Bight and on other Meteorological Parameters. In *Symposium Storm*, 1991.

H. Schmidt and H. von Storch. German Bight Storms Analysed. *Nature*, 365: 791, October 1993.

T. Schmith. Occurence of Severe Winds in Denmark During the Past 100 Years. *Proeedings of the Sixth International Meeting on Statistical Climatology*, pages 83–86, 1995.

C.-D. Schönwiese. *Klimatologie*. UTB, 2008.

Seewarte. *Instruktionen für dir Signalstellen der Deutschen Seewarte*. Deutsche Seewarte, Hamburg, 1876.

Seewarte. *Instruktionen für dir Signalstellen der Deutschen Seewarte*. Deutsche Seewarte, Hamburg, 1880.

Seewarte. *Instruktionen für dir Signalstellen der Deutschen Seewarte*. Deutsche Seewarte, Hamburg, 1889.

Seewarte. *Instruktionen für dir Signalstellen der Deutschen Seewarte*. Deutsche Seewarte, Hamburg, 1902.

Seewarte. *Dienstanweisung für die Sturmwarnungsstellen*. Deutsche Seewarte, Hamburg, 1938.

V. Slonosky, P. Jones, and T. D. Davies. Homogenization Techniques for European Monthly Mean Surface Pressure Series. *Journal of Climate*, 12:2658 – 2672, August 1999.

A. Smits, A. T. Klein, and G. Können. Trends in Storminess over the Netherlands. *International Journal of Climatology*, 25:1331–1344, 2005.

E. Suvilampi. Voimakkaiden geostrofisten tuulten alueellisuus ja muutokset suomessa vuosina 1884-2100. *Pro Gradu-tutkielma. Turun yliopisto, maantieteen laitos.*, 2009.

B. R. Thomas, E. C. Kent, and V. R. Swail. Methods to Homgenize Wind Speeds from Ships and Buoys. *International Journal of Climatology*, 25:979–995, 2005.

B. Tinz, G. Rosenhagen, R. Sedlatschek, H. Otten-Balaccanu, W. Gloeden, and A. Ganske. ERA-Reanalysen für die Qualitätskontrolle maritim-meteorologischer Daten. In *DACH-Tagung*, 2013.

B. Tinz, T. Leiding, R. Sedlatschek, H. Otten-Balaccanu, L. Gates, W. Gloeden, G. Rosenhagen, and D. Röhrbein. Qualitätsprüfung maritim-meteorologischer Daten. Deutscher Wetterdienst, 2015.

S. M. Uppala, P. Kållberg, A. Simmons, U. Andrae, V. d. Bechtold, M. Fiorino, J. Gibson, J. Haseler, A. Hernandez, G. Kelly, et al. The ERA-40 Re-Analysis. *Quarterly Journal of the Royal Meteorological Society*, 131(612):2961–3012, 2005.

H. von Storch and K. Worth. *Sturmfluten*, volume 41. Geschichte-Fachdidaktik-Politische Bildung, 2011.

H. von Storch, W. Jiang, and K. Furmancyk. *Storm Surge Case Studies*, chapter Elsevier Treatise in Hazards and Disasters, pages 181–196. Elsevier, 2015.

D. Wagner, B. Tinz, and H. von Storch. Signal stations: Newly digitized historical climate data of the german bight and the southern baltic sea coast. *Journal of Atmospheric and Oceanic Technology*, 33(12):2735–2741, 2016.

X. L. Wang, F. W. Zwiers, V. R. Swail, and Y. Feng. Trends and Variability of Storminess in the Northeast Atlantic Region, 1874-2007. *Climate Dynamics*, 33:1179–1195, 2009.

X. L. Wang, H. Wan, F. W. Zwiers, V. R. Swail, G. P. Compo, R. J. Allan, R. S. Vose, D. Jourdain, and X. Yin. Trend and Low-Frequenciey Variability of Storminess over Western Europe, 1878-2007. *Climate Dynamics*, 37:2355–2371, 2011.

X. L. Wang, Y. Feng, G. Compo, V. Swail, F. Zwiers, R. Allan, and P. Sardeshmukh. Trends and Low Frequency Variability of Extra-Tropical Cyclone

Activity in the Ensemble of Twentieth Century Reanalysis. *Climate Dynamics*, 40(11-12):2775–2800, 2013a.

X. L. Wang, Y. Feng, G. Compo, F. W. Zwiers, R. Allan, V. R. Swail, and P. Sardeshmukh. Is the Storminess in the Twentieth Century Reanalysis really Inconsistent with Observations? a Reply to the Comment by Krueger et al. (2013b). *Climate Dynamics*, 2013b.

WASA. Changing Waves and Stormes in the Notheast Atlantic? *Bulletin of the American Meteorological Society*, 79:741–760, 1998.

R. Weisse, H. von Storch, and F. Feser. Northeast Atlantic and North Sea Storminess as Simulated by a Regional Climate Model 1958-2001. *Journal of Climate*, 18:465–479, 2005.

R. Weisse, H. von Storch, U. Callies, A. Chrastansky, F. Feser, I. Grabemann, H. Guenther, A. Pluess, T. Stoye, J. Tellkamp, J. Winterfeldt, and K. Woth. Regional Meteorological-Marine Reanalysis and Climate Change Projections: Results for Northern Europe and Potentials for Coastal and Offshore Applications. *Bulletin of the American Meteorological Society*, 90:849–860, 2009.

L. Wern and L. Bärring. *Sveriges vondklimat 1901-2008 - Analys av förädering i geostrofik vind*. SMHI, Norrköpping, Sweden, meteorologi nr 138/2009 edition, 2009.

WMO. WMO International Codes, 2016. URL `http://www.wmo.int/pages/prog/www/WMOCodes.html`.

H. Wulff. Sturmwarnstellen an der Deutschen Küste - das Ende eines über 100 Jahre alten Dienstes. Weather map of the Deutscher Wetterdienst, Deutscher Wetterdienst - Seewetteramt, December 1982.

List of Figures

List of Tables

A Appendix

Table A.1.: List of place names with the country and the geographic coordinates.

Station Name	Country	LON	LAT
Aarosund	Denmark	N55.25	E9.72
Borkum	Germany	N53.35	E6.67
Dornbusch	Germany	N54.58	E13.12
Greetsiel	Germany	N53.50	E7.09
Greifswalder Oie	Germany	N54.25	E13.92
Hamburg	Germany	N53.55	E10.0
Karkeln/Myssowka	Poland	N55.19	E21.26
Palanga	Lithuania	N55.55	E13.41
Sylt	Germany	N54.92	E8.33

Table A.2.: Example of used configuration data for *validat* with the elements, the routine keywords and a description of these keywords.

Element	Keyword	Description
BFT	CHRONO	1 20 1 abs. und proz. Tol./h; abs. Tol/min
BFT	CLIMAT	-1 +1 1.3 Tol. (-/+), factor for var. climat check
BFT	FILPOS	46-47
BFT	FORMRANGE	0-12
BFT	INFO1	wind force Beaufort
BFT	REPEAT	5 8 1.0 Allowed hours with same value.
BFT	UNIT	Beaufort
BFTQB	FILPOS	49-49
DATE	FILPOS	24-31
DATE	INFO1	YearMonthDay (YYYYMMDD)
DD	CHRONO	99 100 50 abs. und proz. Tol./h; abs. Tol/min
DD	FILPOS	40-42
DD	FORMRANGE	00-36,99
DD	INFO1	Wind direction
DD	REPEAT	10 15 1.0 Allowed hours with same value.
DD	UNIT	1/10
DDQB	FILPOS	44-44
EXAMIN	CLIMAT	PPPP,BFT
EXAMIN	FORMAL	LAT,LON,PPPP,DD, BFT
EXAMIN	REPEAT	PPPP,DD,BFT
HOUR	FILPOS	33-34
HOUR	INFO1	Time in whole hours (UTC)
HOUR	UNIT	UTC
IDENT	FILPOS	1-8
IDENT	INFO1	callsign oder Buoynumber
LAT	FILPOS	10-13
LAT	FORMRANGE	-9000-9000
LAT	INFO	Latitude(-90.00 bis +90.00) Süd = neg, Nord = pos
LAT	UNIT	1/100 degree
LATQB	FILPOS	15-15
LON	FILPOS	17-20
LON	FORMRANGE	-18000-18000
LON	INFO	Longitude (-180.00 bis +180.00) West = neg., Ost = pos.
LON	UNIT	1/100 degree
LONQB	FILPOS	22-22
MINUTE	FILPOS	36-37
MINUTE	INFO1	Time in whole minutes
PPPP	CHRONO	60 0 6 (abs. and perc. tol. per hour; abs. Tol. per minute)
PPPP	CLIMAT	-100 +50 1.0 Tol.-/+) and factor for var. by climat check
PPPP	FILPOS	51-55
PPPP	FORMRANGE	8600-10700
PPPP	REPEAT	4 7 1.0 Allowed hours with same value.
PPPP	UNIT	1/10 hPa
PPPPQB	FILPOS	57-57

1	Aaroesund	DEN	DEN00020	55 16	09 42
2	Ahlbeck	GER	GER02440	53 56	14 11
3	Amrum	GER	GER00200	54 38	08 21
4	Apenrade	DEN	DEN00010	55 03	09 25
5	Arkona_Ruegen	GER	GER02320	54 41	13 26
6	Balga	RUS	RUS00070	54 33	19 58
7	Barhoeft	GER	GER02270	54 26	13 02
8	Borkum	GER	GER00020	53 35	06 40
9	Brake	GER	GER00240	53 20	08 29
10	Bremerhaven	GER	GER00300	53 33	08 34
11	Bruesterort	RUS	RUS00040	54 54	19 56
12	Brunsbuettel_Koog	GER	GER00410	53 54	09 08
13	Brunshausen	GER	GER00430	53 38	09 31
14	Buelk	GER	GER02120	54 27	10 12
15	Buesum	GER	GER00370	54 08	08 52
16	Burgstaaken	GER	GER02180	54 25	11 12
17	Carolinensiel	GER	GER00090	53 42	07 49
18	Ceynowa	POL	POL00240	54 46	18 31
19	Chlapowo	POL	POL00220	54 48	18 22
20	Cranz	RUS	RUS00120	54 58	20 29
21	Cuxhaven	GER	GER00360	53 52	08 43
22	Danzig_Neufahrwasser	POL	POL00290	54 24	18 40
23	Darsser_Ort	GER	GER02240	54 28	12 30
24	Dievenow	POL	POL00070	54 01	14 45
25	Dornbusch_Hiddensee	GER	GER02300	54 36	13 07
26	Drawoehnen	RUS	RUS00270	55 31	21 15
27	Eckernfoerde	GER	GER02040	54 28	09 50
28	Elbinger_Fahrwasser	POL	POL00360	54 10	19 24
29	Ellenbogen_Sylt	GER	GER00220	55 03	08 24
30	Emden_Nesserland	GER	GER00060	53 21	07 11
31	Falshoeft	GER	GER02060	54 46	09 58
32	Fischhausen	RUS	RUS00080	54 44	20 01
33	Flensburg	GER	GER02010	54 48	09 26
34	FS_Amrumbank	GER	GER00100	54 33	07 53
35	FS_Ausseneider	GER	GER00180	54 14	08 18
36	FS_Borkumriff	GER	GER00010	53 43	06 23
37	FS_Elbe III	GER	GER00250	53 58	08 30
38	FS_Fehmarnbelt	GER	GER02170	54 36	11 09
39	FS_Fehmarnsund	GER	GER02160	54 24	11 07
40	FS_Weser	GER	GER00130	53 56	07 56
41	Funkenhagen	POL	POL00110	54 14	15 55
42	Geestemuende	GER	GER00320	53 32	08 36
43	Gilge	RUS	RUS00260	55 01	21 14
44	Glueckstadt	GER	GER00420	53 47	09 25
45	Goehren_Ruegen	GER	GER02370	54 20	13 44

Figure A.1.: List of all signal stations with the station number, the name, the country, identification number, longitute and latitude.

46	Gotenhafen	POL	POL00260	54 31	18 33
47	Greetsiel	GER	GER00030	53 30	07 06
48	Greifswalder_Oie	GER	GER02410	54 15	13 55
49	Großendorf	POL	POL00230	54 48	18 24
50	Hamburg	GER	GER00490	53 33	09 59
51	Heiligenbeil_Rosenberg	RUS	RUS00060	54 28	19 56
52	Heiligenhafen	GER	GER02150	54 22	10 59
53	Hela	POL	POL00320	54 37	18 49
54	Helgoland	GER	GER00110	54 11	07 53
55	HH_Altenwerder	GER	GER00460	53 31	09 55
56	HH_Altona	GER	GER00470	53 33	09 56
57	HH_Seefahrtsschule	GER	GER00480	53 32	09 58
58	HH_Seemannshoeft	GER	GER00450	53 32	09 53
59	Hoheweg_Lt	GER	GER00170	53 43	08 15
60	Holnis	GER	GER02030	54 52	09 36
61	Husum	GER	GER00400	54 29	09 03
62	Inse	RUS	RUS00250	55 07	21 13
63	Jershoeft	POL	POL00140	54 32	16 33
64	Kahlberg	POL	POL00370	54 23	19 27
65	Kamp_Karnin	GER	GER02400	53 51	13 51
66	Kappeln	GER	GER02050	54 40	09 56
67	Karkelbeck	RUS	RUS00190	55 50	21 05
68	Karkeln	RUS	RUS00280	55 12	21 16
69	Karwen	POL	POL00200	54 50	18 13
70	Keitum_Sylt	GER	GER00210	54 54	08 22
71	Kiel_Binnenhafen	GER	GER02080	54 19	10 09
72	Kiel_Friedrichsort	GER	GER02110	54 24	10 11
73	Kiel_Lindenauhafen	GER	GER02090	54 23	10 10
74	Kiel_Wellingdorf	GER	GER02100	54 19	10 10
75	Kolbergermuende	POL	POL00100	54 11	15 34
76	Koserow	GER	GER02420	54 03	14 01
77	Kussfeld	POL	POL00280	54 44	18 35
78	Kuwertshof	RUS	RUS00300	55 21	21 19
79	Labagienen	RUS	RUS00290	54 59	21 16
80	Leba	POL	POL00170	54 46	17 33
81	Lenzen	POL	POL00380	54 16	19 28
82	List_Sylt	GER	GER00230	55 01 07	08 26 31
83	Luebeck	GER	GER02130	53 52	10 41
84	Marienleuchte_Fehmarn	GER	GER02190	54 30	11 14
85	Meierwik	GER	GER02020	54 49	09 30
86	Mellneraggen	RUS	RUS00210	55 44	21 06
87	Memel	RUS	RUS00220	55 43	21 07
88	Misdroy	POL	POL00020	53 56	14 27
89	Munkmarsch_Sylt	GER	GER00190	54 55	08 21
90	Nest	POL	POL00120	54 16	16 05
91	Neu_Terranova	POL	POL00350	54 13	19 22
92	Neuendorf_Hiddensee	GER	GER02290	54 32	13 06
93	Neuendorf_Kiesberg	POL	POL00050	53 59	14 35
94	Neufaehr	POL	POL00310	54 21	18 47
95	Neuharlinger_Siel	GER	GER00080	53 42	07 42
96	Neukrug	POL	POL00390	54 27	19 37
97	Neukuhren	RUS	RUS00100	54 57	20 14
98	Neuwerk	GER	GER00260	53 55	08 30
99	Nidden	RUS	RUS00160	55 18	21 00
100	Nimmersatt	RUS	RUS00170	55 52	21 04
101	Norddeich	GER	GER00050	53 37	07 10

Figure A.2.: List of all signal stations with the station number, the name, the country, identification number, longitute and latitude.

102	Norderney	GER	GER00040	53 42	07 09
103	Oevenum_ Foehr	GER	GER00280	54 43	08 32
104	Oldersum	GER	GER00070	53 20	07 21
105	Ost_Deep	POL	POL00090	54 09	15 18
106	Ostesperrwerk	GER	GER00390	53 49	09 02
107	Oxhoeft	POL	POL00250	54 33	18 33
108	Palmnicken	RUS	RUS00050	54 52	19 56
109	Peenemuende	GER	GER02390	54 09	13 46
110	Pellworm	GER	GER00350	54 31	08 42
111	Peyse	RUS	RUS00090	54 40	20 06
112	Pfahlbude	RUS	RUS00010	54 26	19 45
113	Pillau	RUS	RUS00030	54 39	19 53
114	Pillau II	RUS	RUS00020	54 39	19 52
115	Pillkoppen	RUS	RUS00150	55 14	20 56
116	Putziger_Heisternest	POL	POL00300	54 42	18 41
117	Rechtenfleth	GER	GER00270	53 23	08 31
118	Rinderort	RUS	RUS00180	54 54	21 04
119	Rixhoeft	POL	POL00210	54 50	18 20
120	Rossitten	RUS	RUS00140	55 09	20 51
121	Rostock	GER	GER02230	54 05	12 07
122	Ruden	GER	GER02380	54 12	13 46
123	Ruegenwaldermuende	POL	POL00130	54 25	16 24
124	Sarkau	RUS	RUS00130	55 01	20 37
125	Sassnitz_Ruegen	GER	GER02340	54 31	13 39
126	Schiewenhorst	POL	POL00330	54 20	18 56
127	Schillighoern	GER	GER00140	53 42	08 02
128	Schleimuende	GER	GER02070	54 40	10 01
129	Scholpin	POL	POL00160	54 43	17 15
130	Schwarzort_Duene	RUS	RUS00230	55 33	21 07
131	Seebad_Foersterei	RUS	RUS00200	55 46	21 05
132	Seebad_Horst	POL	POL00080	54 06	15 05
133	Stadersand	GER	GER00440	53 37	09 32
134	Stettin	POL	POL00040	53 26	14 33
135	Stilo	POL	POL00180	54 47	17 44
136	Stolpmuende	POL	POL00150	54 35	16 52
137	Stralsund	GER	GER02280	54 19	13 05
138	Stubbenkammer_Ruegen	GER	GER02350	54 34	13 40
139	Suederhoeft	GER	GER00340	54 17	08 41
140	Swinemuende	POL	POL00010	53 55	14 15
141	Thiessow	GER	GER02360	54 17	13 43
142	Timmendorf_auf_Poel	GER	GER02200	53 59	11 23
143	Toenning	GER	GER00380	54 19	08 57
144	Travemuende	GER	GER02140	53 58	10 53
145	Ueckermuende	GER	GER02430	53 45	14 04
146	Vierow	GER	GER02330	54 06	13 34
147	Vogelsang	POL	POL00340	54 21	19 17
148	Wangerooge	GER	GER00120	53 47	07 54
149	Warnemuende	GER	GER02220	54 11	12 05
150	Wehrdamm	RUS	RUS00110	54 41	20 23
151	Weser_Lt	GER	GER00160	53 52	08 08
152	Wesermuende	GER	GER00310	53 32	08 35
153	Westerhever	GER	GER00330	54 23	08 40
154	Wieck	GER	GER02250	54 25	12 35
155	Wilhelmshaven	GER	GER00150	53 31	08 06
156	Windenburg	RUS	RUS00240	55 21	21 12
157	Wismar	GER	GER02210	53 54	11 28

Figure A.3.: List of all signal stations with the station number, the name, the country, identification number, longitute and latitude.

158	Wittenberg	POL	POL00190	54 49	17 58
159	Wittower_Posthaus	GER	GER02310	54 34	13 11
160	Wollin	POL	POL00060	53 51	14 37
161	Wyk_Foehr	GER	GER00290	54 41	08 34
162	Ziegenort	POL	POL00030	53 40	14 31
163	Zingst	GER	GER02260	54 26	12 41
164	Zoppot	POL	POL00270	54 27	18 34

Figure A.4.: List of all signal stations with the station number, the name, the country, identification number, longitute and latitude.

Publication

D. Wagner, B. Tinz, H. von Storch. Signal Stations: Newly Digitized Historical Climate Data of the German Bight and the southern Baltic Sea Coasts. *JTECH*, 2016, doi: http://dx.doi.org/10.1175/JTECH-D-15-0199.1.

Acknowledgment

First of all, my grateful thanks go to Dr. Birger Tinz, my supervisor and Prof. Dr. Hans von Storch for his supervision, help, time and support. I also want to thank Prof. Dr. Heinke Schlünzen for his support as my panel chair.
I am thankful for my position at the German Meteorological Service (DWD) in Hamburg and I would like to thank Gudrun Rosenhagen for their inducement to digitize and analyze the signal station data. My special thanks goes to all employees of the DWD, who digitized the signal station data by hand and Dr. Lydia Gates, head of KU24, for her improvement proposals. I also want to thank Martin Stendel of the DMI to made the data of Hammer Odde station available.
I would like to thank my roommate Tina Leiding for scientific discussions and having fun in everyday work.
Furthermore, I am thankful for being a PhD student at the School of Integrated Climate System Sciences (SICSS) of CliSAP in Hamburg.
Many thanks go to Sonja Drüke for proof-reading this work and to Dr. Manuela Sauer for her supportive words.
Special thanks go to my parents, my family and friends for their belief in me and to Simon for every day support.

Eidesstattliche Erklärung

Hiermit erkläre ich an Eides statt, dass ich die vorliegende Dissertationsschrift selbst verfasst und keine anderen als die angegebenen Quellen und Hilfsmittel benutzt habe.

Hamburg, den 30.10.2017